Characterizing biological nitrification inhibition using native *Nitrosomonas europaea*: mechanism studies and maize cultivar screening

by

Lauren Elizabeth Stanton

B.S., Kansas State University, 2024

A THESIS

submitted in partial fulfillment of the requirements for the degree

MASTER OF SCIENCE

Carl and Melinda Helwig Department of Biological and Agricultural Engineering
Carl R. Ice College of Engineering

KANSAS STATE UNIVERSITY
Manhattan, Kansas

2025

Approved by:

Co-Major Professor
Dr. Trisha Moore

Approved by:

Co-Major Professor
Dr. Jeongdae Im

Copyright

© LaurenStanton2025.

Abstract

The nitrogen-use efficiency (NUE) of agricultural plants is notoriously poor, typically ranging from 30 to 50%. Ideally, nitrogen (N) fertilizers, primarily applied as ammonium (NH_4^+), would remain stable to allow optimal uptake by plants. However, NH_4^+ is rapidly transformed within the soil through a microbial process called nitrification. In this process, ammonia-oxidizing bacteria (AOB), such as *Nitrosomonas europaea*, oxidize NH_4^+ and ammonia (NH_3) to nitrite (NO_2^-), which is further converted to nitrate (NO_3^-) by nitrite-oxidizing microorganisms and eventually reduced to di-nitrogen (N_2) via denitrification. These processes release nitrous oxide (N_2O) as a by-product, accounting for up to three-quarters of total anthropogenic N_2O emissions in the U.S. N_2O is the third most potent greenhouse gas (GHG) and is also the leading ozone-depleting substance. Therefore, mitigating nitrification is crucial for reducing the environmental impact of agriculture. Recent research has demonstrated that certain plants release phytochemicals through their roots to suppress nitrification, a phenomenon called Biological Nitrification Inhibition (BNI). BNI chemicals disrupt the enzymatic pathways required for nitrification; however, the precise inhibition mechanisms and their impacts on *N. europaea* remain poorly understood. Previous studies have primarily focused on quantifying BNI activity using recombinant bioluminescent *N. europaea* due to its heightened sensitivity compared to native strains. However, recombinant strains may not fully represent the behavior and responses of nitrifiers in natural environments. Moreover, their use complicates direct comparisons of BNI effects across studies and conditions, as genetic modifications can introduce confounding factors that do not reflect natural microbial responses. In this study, I systematically evaluated the half-maximal inhibitory concentration (IC_{50}) values and inhibition mechanisms of selected, structurally diverse authentic BNIs including 1,9-Decanediol (1,9-D), Methyl 3-(4-

hydroxyphenyl) propionate (MHPP), and Linoleic Acid (LA) on native *N. europaea* under standardized assay conditions. Synthetic nitrification inhibitor, Allylthiourea (AT), was used as a reference compound. To further expand the application of BNI research beyond microbial studies, I extended my research to maize, aiming to integrate BNI traits into the major agricultural crop. Given that BNI activity varies among plant species and even among cultivars, this study was focused on maize, a significant global crop with substantial potential to improve NUE through targeted breeding. I optimized the BNI activity screening protocol for plants and applied it to evaluate 100 maize germplasm lines, with the goal of identifying cultivars exhibiting the highest BNI activity. By linking physiological traits to BNI potential, this approach lays the groundwork for translating fundamental research into practical applications in agriculture, ultimately supporting the development of sustainable practices that enhance NUE and reduce environmental impact.

Table of Contents

Table of Contents v
List of Abbreviations and Acronyms ix
List of Figures x
List of Tables xii
Acknowledgements xiii
Dedication xiv
Chapter 1 - The Nitrogen Cycle and Biological Nitrification Inhibition: A Review 1
Introduction 1
The Nitrogen Cycle 1
Excessive Nitrogen Use and Its Environmental Impact 3
Current Methods for Nitrification Control 4
Biological Nitrification Inhibition 6
Thesis Objectives 9
Chapter 2 - Characterization and Quantification of BNI Activity (IC_{50} and Reversibility) with native *N. europaea* 10
Abstract 10
Introduction 10
Materials and Methods 12
General Setup and Culture Conditions 12
Gen.1a. Bacterial strain and growth conditions 12
Gen.1b. NO_2^- Quantification 13
Gen.1c. Cell harvesting and preparation 14
Gen.1d. Chemicals 14
Experiment 1: Determination of the Nitrification IC_{50} 14
Experiment 1a. IC_{50} Assay Setup 14
Experiment 1b. Inhibition Calculation 15
Experiment 1c. IC_{50} Model 16
Experiment 2: Reversibility of Inhibition 17
Experiment 2a. Inhibition Exposure and Initial Monitoring 17

Experiment 2b. Post-Exposure Monitoring and Reversibility Assessment 17
Results and Discussion 18
Bacterial Growth and NO_2^- Production 18
Determination of IC_{50} 19
Individual Compound Inhibition Profiles 20
AT: Potent Inhibitor Across Biomass Concentrations 20
1,9-D: Biomass-Dependent Inhibitor 21
MHPP: Potent Inhibitor with Minimal Biomass Impact 22
LA: Ineffective Inhibitor with Low Solubility 23
Inhibition Patterns 24
Reversibility of Inhibition 25
Comparison with Existing Research 28
Limitations 32
Future Research 33
Conclusions 34
Chapter 3 - Transcriptomic Response of *N. europaea* Upon Exposure to BNI Compounds 36
Abstract 36
Introduction 36
Overview of Gene Expression and Ribonucleic Acid (RNA) 37
Genes Associated with Nitrification 37
Materials and Methods 38
General Setup and Culture Conditions 38
Experiment 1: Preliminary Timing for RNA Extraction 38
Experiment 1a. Incubation Setup 38
Experiment 1b. RNA Extraction 39
Experiment 1c. Quantitative Polymerase Chain Reaction (qPCR) Analysis 40
Experiment 2: Final RNA Extraction and Transcriptome Sequencing 40
Experiment 2a. Incubation and Sampling 40
Experiment 2b. RNA Extraction 41
Experiment 2c. Quantitative Polymerase Chain Reaction (qPCR) Analysis 41
Experiment 2d. RNA Sequencing and Annotation 41

Results and Discussion 41
Physiological Responses to BNI Compounds 41
Transcriptional Responses to BNI Compounds 42
Hypothesized Impact of Inhibitors on Gene Expression 44
Conclusions 45
Chapter 4 - Screening Maize Cultivars for Biological Nitrification Inhibition Activity 46
Abstract 46
Introduction 47
Maize Growth Stages and N Demand 47
BNI Potential in Maize 48
BNI Capacity and Success in Wheat 49
Our Screening Protocol 50
Materials and Methods 50
General Setup and Culture Conditions 50
Experiment 1: Protocol Optimization for BNI Screening 50
Experiment 1a. Initial Experimental Setup 51
Experiment 1b. Screening Cultivars 52
Experiment 2: Optimized Protocol for BNI Screening 53
Experiment 2a. Hydroponic Cultivation of Maize Cultivars 53
Experiment 2b. Screening Cultivars 54
Experiment 2c. Conversion to AT Units 55
Experiment 2d. Statistical Analysis 56
Results and Discussion 56
BNI Screening Protocol Optimization 56
Effect of Scaling Down to 96-Well Microplates (Iteration 1) 56
Effect of Washing Cells Prior to Screening (Iteration 2) 58
Effect of Stop Solution Addition (Iteration 3) 59
Effect of Increasing Target Optical Density (Iteration 4) 60
Effect of Maize Hydroponic System (Iteration 5) 61
Final Optimized Protocol Performance 63
Comparison to Existing Methods 63

BNI Capacity in Maize Cultivars Across Growth Stages 64
Limitations and Sources of Error 66
Future Research 67
Conclusions 67
Chapter 5 - Overall Discussion and Conclusion 69
References 72

List of Abbreviations and Acronyms

AMO	Ammonia Monooxygenase
AOB	Ammonia-oxidizing Bacteria
AT	Allylthiourea
BNI	Biological Nitrification Inhibition
cDNA	Complementary DNA
DCD	Dicyandiamide
DI	Deionized
DMPP	Dimethylpyrazole phosphate
DMSO	Dimethyl sulfoxide
g	Gravity, 9.81 m/s^2
GHG	Greenhouse Gas
HAO	Hydroxylamine Oxidoreductase
IC_{10}	Concentration responsible for 10% nitrification inhibition
IC_{50}	Concentration responsible for 50% nitrification inhibition
LA	Linoleic Acid
MHPP	Methyl 3-(4-hydroxyphenyl) propionate
mRNA	Messenger RNA
N	Nitrogen
N_2O	Nitrous Oxide
NH_2OH	Hydroxylamine
NH_3	Ammonia
NH_4^+	Ammonium
NO	Nitric Oxide
NO_2^-	Nitrite
NO_3^-	Nitrate
NOB	Nitrite-oxidizing bacteria
NUE	Nitrogen Use efficiency
OD_{600}	Optical Density at 600 nm
PCR	Polymerase Chain Reaction
qPCR	Quantitative Polymerase Chain Reaction
RCF	Relative Centrifugal Force
RNA	Ribonucleic Acid
SNI	Synthetic Nitrification Inhibitor

List of Figures

Figure 1.1. Microbial N cycle and NUE. 2

Figure 1.2. U.S. greenhouse gas emissions (Sands, 2024). 4

Figure 2.1. Standard curve for NO_2^- quantification. 18

Figure 2.2. Dose-response curves of Allylthiourea (AT) on nitrite production inhibition by *N. europaea* at various OD_{600} values.. 20

Figure 2.3. Dose-response curves of 1,9-Decanediol (1,9-D) on nitrite production inhibition by *N. europaea* at various OD_{600} values. 21

Figure 2.4. Dose-response curves of Methyl 3-(4-hydroxyphenyl) propionate (MHPP) on nitrite production inhibition by *N. europaea* at various OD_{600} values. 22

Figure 2.5. Dose-response curves of Linoleic Acid (LA) on nitrite (NO_2^-) production inhibition by *N. europaea* at various OD_{600} values.. 24

Figure 2.6. Reversibility of Inhibition in *N. europaea* for selected compounds - nitrite production over time. 27

Figure 3.1. Nitrite Inhibition in RNA Extraction Sample. 42

Figure 3.2. *amoA*/16S Ratio in RNA Extraction Sample. 43

Figure 4.1. Corn Growth and Development (Ciampitti et al., 2016). 48

Figure 4.2. Scaffold System Setup for Maize Cultivation.. 52

Figure 4.3. Hydroponic System Setup and Root Biomass. 54

Figure 4.4. Comparison between 50-mL flask and 96-well microplate BNI screening methods..57

Figure 4.5. Impact of wash step on initial NO_2^- concentration. 59

Figure 4.6. Visible biomass after centrifugation.. 61

Figure 4.7. Significant root biomass from updated hydroponic system.. 62

Figure 4.8. Algal contamination from hydroponic system.. 63

Figure 4.9. ATU of maize cultivars at various growth stages. 65

List of Tables

Table 1.1. Biological Nitrification Inhibitors 7

Table 2.1. Summary of IC_{50} Values 19

Table 2.2. Comparison of IC_{50} values between bioluminescent and native *N. europaea*. 28

Appendix Table C.1. Primer Information 85

Appendix Table D.1. KSU17 and B104 Summary for 28, 30, and 45 days. 86

Appendix Table D.2. KSU17 and B104 Summary for 21, 28, 30, and 45 days. 86

Acknowledgements

I would like to sincerely thank the many individuals and organizations who have supported me throughout the completion of this thesis. First and foremost, my deepest appreciation goes to my research advisor, Dr. Jeongdae Im, for the guidance and expertise provided throughout this journey. Thank you for pushing me and helping me grow through this experience. I am grateful for all your insights and feedback.

I would also like to thank members of my master's committee—Dr. Trisha Moore and Dr. Sonny Lee—for their suggestions and commitment to this work. I am very grateful for your insights and expertise.

I am also very grateful for my fellow lab mates in the Environmental Biotechnology Lab, Seongmin Yang, Fuhad Hasan Fahim, and Pratap Bikram Shahi. You all have been so supportive and understanding on this journey. I am incredibly thankful for all the coffee runs, conversations, and the encouragement throughout this journey. Thank you to the Radina's coffeeshop in the Carl R. Ice College of Engineering Complex for the liquid motivation.

Additionally, support for this research was provided by the Kansas NSF EPSCoR RII Track-1 Award OIA-1656006 and NSF Award 2144189 (JI).

Dedication

To my Lord and Savior, Jesus Christ, whose steadfast love and peace have carried me through every challenge and triumph in this journey. To my family and friends, whose unwavering support and encouragement have been crucial to my success and journey. Thank you for believing in me.

Chapter 1 - The Nitrogen Cycle and Biological Nitrification Inhibition: A Review

Introduction

The global population is projected to reach 9.7 billion by 2050, intensifying the demand for food production and placing immense pressure on agricultural systems to maximize crop yields while minimizing environmental impacts (*Population | United Nations*, 2024). To sustain crop productivity, producers rely on nitrogen-based fertilizers, as nitrogen (N) is an essential nutrient for plant growth and a key driver of global food production. However, inefficiencies in the N cycle result in significant losses through leaching, runoff, and gaseous emissions, ultimately reducing nitrogen use efficiency (NUE) and contributing to environmental concerns (Fowler et al., 2013; X. Yu et al., 2022). To balance agricultural productivity and sustainability, it is crucial to understand the N cycle and develop strategies to improve NUE. This review explores the N cycle, the link between nitrous oxide (N_2O) emissions and agriculture, existing methods for nitrification control, and the emerging potential of Biological Nitrification Inhibition (BNI) as a sustainable solution.

The Nitrogen Cycle

N is a fundamental element for plant growth and agricultural productivity, yet its inefficient utilization leads to significant environmental and economic challenges. The N cycle is heavily influenced by microbial processes, particularly nitrification and denitrification. Nitrification is the biological oxidation of ammonium (NH_4^+) or ammonia (NH_3) in to nitrate (NO_3^-) (Figure 1.1). This process occurs in two steps: first, ammonia-oxidizing bacteria (AOB) convert NH_3 into nitrite (NO_2^-), followed by nitrite-oxidizing bacteria (NOB) further oxidizing

NO_2^- into NO_3^- (Li et al., 2022). Common soil AOBs include the genera *Nitrosomonas* and *Nitrosospira* within the β-proteobacteria family (Kowalchuk & Stephen, 2001). These microorganisms play a crucial role in the N cycle. While nitrification appears straightforward, it involves complex biochemical steps. The first step includes NH_4^+ oxidation to hydroxylamine (NH_2OH) by the membrane-bound ammonia monooxygenase (AMO), followed by NH_2OH oxidation to NO_2^- via periplasmic hydroxylamine oxidoreductase (HAO) (Kowalchuk & Stephen, 2001; Li et al., 2022). Subsequently, NOB convert NO_2^- into NO_3^- for plants to uptake (Li et al., 2022).

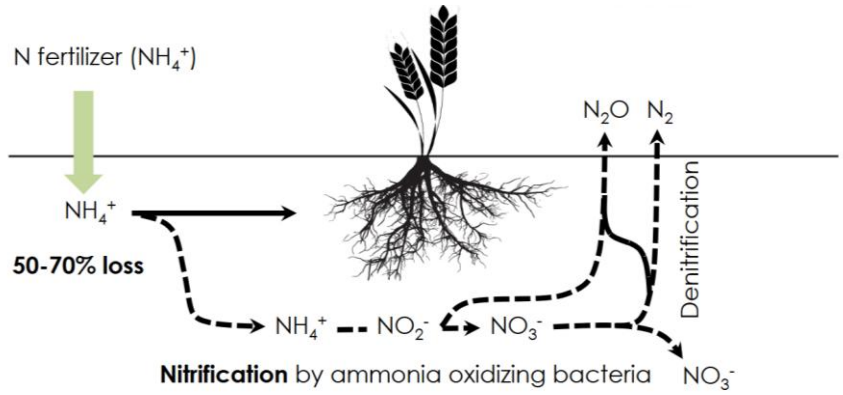

Figure 1.1. Microbial N cycle and NUE. This diagram illustrates the key microbial processes involved in nitrification and denitrification, emphasizing their roles in nitrogen transformations and nitrogen fertilizer efficiency.

Once formed, NO_3^- is highly mobile in the soil and susceptible to leaching into groundwater, thereby reducing N availability for crops. Additionally, NO_3^- can undergo denitrification, a process in which NO_3^- is converted into N gases, including N_2O—a potent greenhouse gas and ozone-depleting substance. These N losses not only reduce fertilizer efficiency, but also contribute to significant environmental issues.

Excessive Nitrogen Use and Its Environmental Impact

N fertilizers are extensively used in agriculture to maximize crop yields and ensure global food production. Despite this substantial input, the NUE of most crops remains low, ranging from 30% to 50% (Li et al., 2022; Wang et al., 2021), leading to significant N losses to the environment. To compensate for this inefficiency, producers often apply excess fertilizer to safeguard yield potential. However, this practice not only increases production costs but also leads to unintended environmental consequences.

Excessive fertilizer application exacerbates N losses through nitrification and denitrification, both of which release N_2O as a by-product. Combined with other aspects of agricultural soil management, these microbial processes are responsible for up to 75% of total anthropogenic N_2O emissions in the United States (*Nitrous Oxide Emissions | US EPA*, 2025). As a result, N_2O from agricultural soils contributes approximately 309.1 million metric tons (MMT) of CO_2-equivalent emissions, as seen below in Figure 1.2 (Sands, 2024). N_2O is not only the leading ozone-depleting substance, but also one of the most potent GHGs (Fowler et al., 2013), making it a significant environmental threat. Moreover, the nitrification process increases NO_3^- leaching into the groundwater and surface waters, which can contaminate drinking water and fuel harmful algal blooms (Erisman et al., 2013; Penuelas et al., 2023). Elevated NO_3^- exposure has been associated with various human health risks—such as certain cancers, upper respiratory illnesses, immune disfunction, and methemoglobinemia ("blue baby syndrome")—underscoring the broader public-health implications of excessive fertilizer use (Erisman et al., 2013; Penuelas et al., 2023). Given these widespread impacts, effective N management is essential for reducing N losses, mitigating environmental damage, reducing human health impacts, and improving agricultural sustainability.

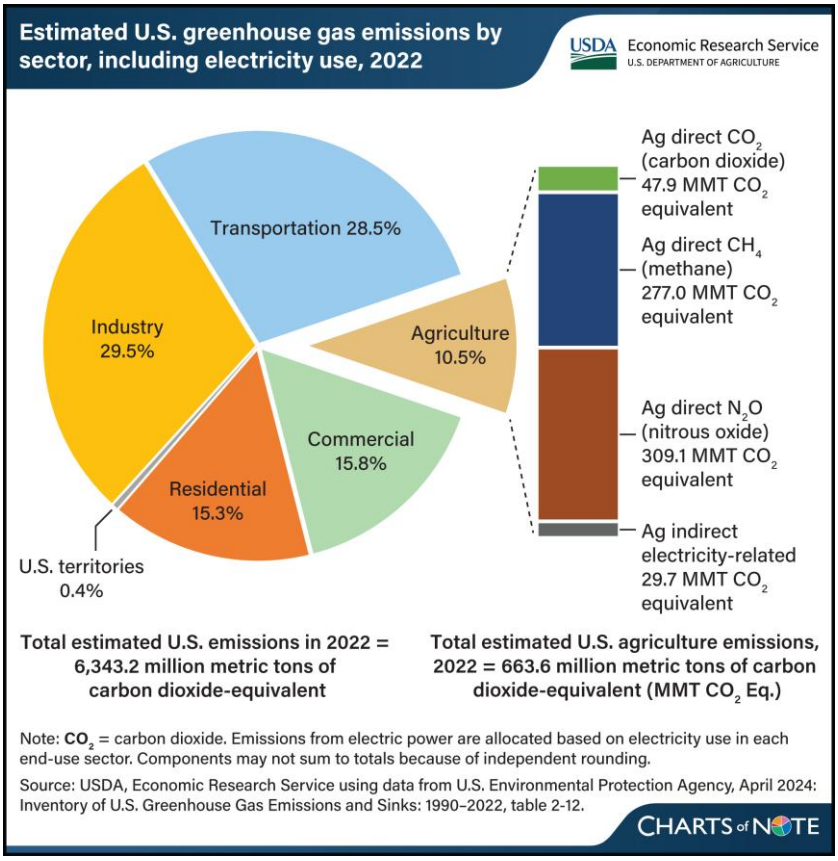

Figure 1.2. U.S. greenhouse gas emissions (Sands, 2024). This chart displays the distribution of greenhouse gas emissions in the United States, highlighting that agriculture is responsible for 10.5% of total U.S. emissions. Within agriculture, 309.1 MMT CO_2 equivalent is emitted as nitrous oxide (N_2O).

Current Methods for Nitrification Control

Managing nitrification within the soil is a key strategy for improving NUE and reducing environmental impacts in agricultural systems. Current approaches to nitrification control include the 4R Nutrient Stewardship, adapted fertilizers, and synthetic nitrification inhibitors (SNIs), each offering varying degrees of effectiveness in minimizing N losses.

The 4R Nutrient Stewardship, a widely adopted framework, emphasizes applying the right fertilizer source at the right rate at the right time and in the right place. Precision agriculture

technologies enhance this approach by targeting fertilizer application directly in the root zone, reducing leaching and runoff (Penuelas et al., 2023). Another example of 4R management is split N applications, where fertilizer is applied throughout the growing season, rather than applying all at once. However, the success of 4R strategies depend on site-specific factors, weather conditions, farmer adoption, and the access to precision technologies.

Beyond proper fertilization management, researchers are exploring adapted fertilizers to enhance N retention and availability. These include slow-release fertilizers, organic waste-based resource fertilizers, urea super granules, and microbial agent and algae-based biofertilizers (Kumar et al., 2015; Li et al., 2022). While these technologies have demonstrated reductions in N losses, further research is needed to facilitate their real-world implementation. Many remain in early development stages, and factors such as cost and ease of implementation require further evaluation (Li et al., 2022). Despite the promise of these emerging fertilizers, their widespread adoption remains limited.

Another approach to nitrification management is the use of synthetic nitrification inhibitors (SNIs)—man-made compounds designed to slow nitrification by suppressing AOBs. The first commercial SNI, Nitrapyrin (2-chloro-6-(trichloromethyl) pyridine), was introduced to the agricultural market in 1974 (Woodward et al., 2021). Since then, many other SNIs have been developed. Among them, 3,4-dimethylpyrazole phosphate (DMPP) and Dicyandiamide (DCD) are the most widely used (Woodward et al., 2021). While these compounds can reduce nitrification, their high cost, variable effectiveness across environments, and potential environmental toxicity toxicity—both during manufacture and in the soil—raise concerns (Kumar et al., 2015; Woodward et al., 2021). Given these limitations, SNIs are not a viable long-

term solution. Their drawbacks have fueled interest in more sustainable alternatives to enhance NUE and reduce N losses.

Biological Nitrification Inhibition

Fortunately, nature already offers a solution to improving NUE. Recent studies have established that certain plants can release phytochemicals, known as Biological Nitrification Inhibitors (BNIs), through their roots to impede nitrification. Similar to SNIs, these BNIs hinder the proper functioning of enzymes required for nitrification, such as AMO and HAO. The presence of BNIs was first confirmed in 2009 in the tropical grass *Brachiaria humidicola*, marking the beginning of a new era in nitrification research (Subbarao et al., 2009). This discovery built on earlier work that, in 2006, introduced the use of recombinant bioluminescent *Nitrosomonas europaea*—a bacterium that emits bioluminescence when active—to assess nitrification inhibition (Subbarao, Ishikawa, et al., 2006). This approach has been instrumental in detecting and quantifying BNI activity in plant systems. Since the first reports of BNI in *Brachiaria humidicola* in 2009, BNI activity has been found in several crops, including rice (*Oryza sativa*), sorghum (*Sorghum bicolor*), pearl millet (*Pennisetum glaucum*), and peanut (*Arachis hypogaea*) (Ishikawa et al., 2003; Pariasca Tanaka et al., 2010; Subbarao et al., 2007; Zakir et al., 2008). BNIs have been successfully extracted and isolated from the root tissues and exudates of several plant species, and ongoing research has focused on their characterization (Table 1.1). While progress has been made, many questions remain.

Table 1.1. Biological Nitrification Inhibitors

Chemical Category	Compound	Plant Species	Molecular Structure	Mode of Action
Fatty alcohols	1,9-Decanediol	*Oryza sativa*	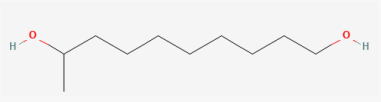	AMO
Fatty acids	Linoleic Acid	*Brachiaria humidicola*	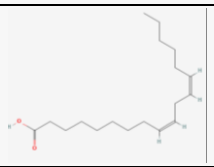	AMO, HAO
	Linolenic Acid	*Brachiaria humidicola*	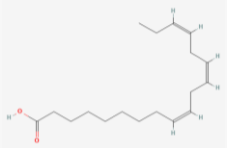	AMO, HAO
Flavanones	Sakuranetin	*Sorghum bicolor*	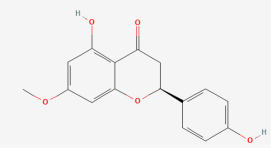	AMO, HAO
Phenolics	Methyl 3-(4-hydroxyphenyl) propionate	*Sorghum bicolor*	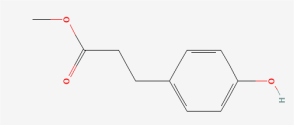	AMO
	Methyl p-coumarate	*Brachiaria humidicola*	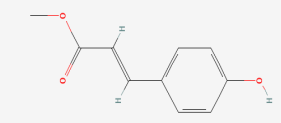	?
	Methyl ferulate	*Brachiaria humidicola*	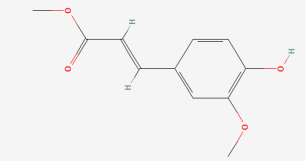	?
	Caffeic Acid	*Nicotiana tobaccum*	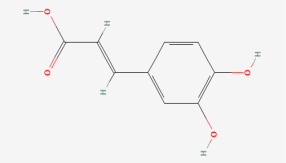	?

Chemical Category	Compound	Plant Species	Molecular Structure	Mode of Action
Phenolics	p-hydroxybenzoic Acid	*Oak species*	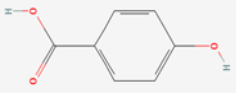	?
	Gallic Acid	*Oak species*	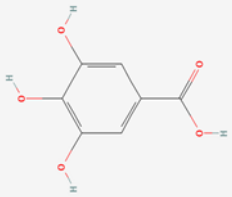	?
	Curcumin	?	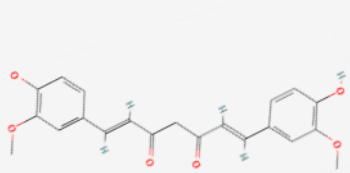	?
	Catechin	*Arbutus unedo*	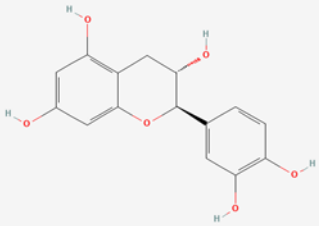	?
Terpenes	Limonene	*Redwood*	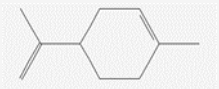	?
	a-phellandrene	*Redwood*	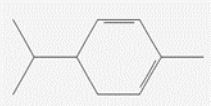	?

? = Unknown

Thesis Objectives

This thesis is guided by several key objectives: first, to quantify BNI potency by determining the half-maximal inhibitory concentration (IC_{50}) and reversibility of various BNI compounds under optimized assay conditions; second, to explore the genetic responses of *N. europaea* when exposed to BNIs; third, to evaluate maize for BNI potential by screening diverse cultivars; and, fourth, to refine and streamline the inhibition assay and screening protocol to improve resource and time efficiency without sacrificing sensitivity. Addressing these objectives will be critical for optimizing the use of BNIs in agricultural systems and developing more sustainable fertilizers, seed treatments, and land management strategies that enhance NUE and environmental sustainability.

Chapter 2 - Characterization and Quantification of BNI Activity (IC_{50} and Reversibility) with native *N. europaea*

Abstract

BNI plays a crucial role in regulating N transformations, yet the inhibitory mechanisms and permanence of BNI compounds remain poorly understood. This study examines the inhibitory potency and reversibility of three BNI compounds—1,9-Decanediol (1,9-D), Methyl 3-(4-hydroxyphenyl) propionate (MHPP), and Linoleic Acid (LA)—using native *N. europaea*, with Allylthiourea (AT), a SNI, included as a reference. The half-maximal inhibitory concentration (IC_{50}; IC_{10} for LA) was determined by exposing cultures on a 96-well microplate to a gradient of inhibitor concentrations and quantifying nitrite (NO_2^-) production, which serves as an indicator of nitrification activity. To assess reversibility, cells were subjected to a washing process following BNI exposure, and their nitrification activity was monitored over time. At an optical density measured at 600 nm (OD_{600}) equal to 0.1, the estimated IC_{50} (or IC_{10} for LA) values for the compounds were: AT = 0.18 µM, 1,9-D = 2,700 µM, MHPP = 368 µM, and LA = 60 µM. In terms of reversibility, *N. europaea* regained activity upon removal of AT, 1,9-D, MHPP, and LA, indicating temporary or reversible inhibition. These findings contribute to a deeper understanding of BNI dynamics and their potential implication for N management strategies.

Introduction

BNI plays a critical role in regulating N transformations by limiting NH_4^+ oxidation. However, discrepancies in existing research hinder a comprehensive understanding of BNI, particularly regarding the potency and mechanisms of inhibition. One major challenge arises

from differences in the test organisms used for evaluation. Many BNI studies have been conducted by a single research group using recombinant bioluminescent *N. europaea*, which, due to its genetic modifications, is highly sensitive to BNIs. This bioluminescent strain carries a plasmid containing *luxAB* genes (Subbarao, Ishikawa, et al., 2006), which allows the bacterium to produce bioluminescence when active. In contrast, native *N. europaea* may exhibit greater resilience than its bioluminescent counterpart, potentially leading to inconsistent inhibition thresholds. Moreover, because this bioluminescent strain is not commercially available or widely distributed by the Subbarao lab group, independent lab groups cannot easily replicate or validate the published data. Together, these factors undermine the reproducibility and applicability of current BNI research.

Beyond biological variations, inconsistencies in experimental methodologies further complicate comparisons across studies. Differences in target biomass (OD_{600}) can influence the interpretation of inhibitory effects. For example, Otaka et al. (2023) utilized bioluminescent *N. europaea* at an OD_{660} of 1.0, while Subbarao, Ishikawa, et al. (2006) did not specify an OD_{600} value, but utilized a 7-day-old culture. In contrast, O'Sullivan et al. (2017) conducted experiments with 10^8 cells mL^{-1}. The variation in biomass concentration can under- and overestimate the IC_{50} values of BNI compounds. Additionally, the final reaction volumes varied across studies with Otaka et al. (2023) conducting experiments in 50-mL amber glass vials with a final reaction volume of 22 mL and Subbarao, Ishikawa, et al. (2006) conducting experiments in test tube with a final reaction volume of 450 µL. As a result, the ratio between BNI compound volume and bacterial suspension volume varied substantially, ranging from 0.004 (1 µL:250 µL [Otaka et al., 2023]) to 0.02 (5 µL:250 µL [Subbarao et al., 2006]) and 0.1 (2 mL:20 mL [O'Sullivan et al., 2017]), impacting the observed inhibitory effects. Another noticeable

inconsistency throughout studies is the exposure time. Otaka et al. (2023) and O'Sullivan et al. (2017) measured NO_2^- after 1 hour incubation with inhibitors, using this time point to determine inhibition. However, Subbarao, Ishikawa, et al. (2006) employed a two-step incubation process: a 30-minute pre-incubation in the dark for bacteria to regain activity after centrifugation followed by a 30-minute incubation period with the inhibitors. Given that bacterial response to inhibitors or solution stabilization may take time, variations in incubation duration or procedure may influence observed inhibitory effects. These methodological differences highlight the need for a standardized approaches to accurately assess BNI effectiveness.

This chapter aims to address these inconsistencies by systematically characterizing and quantifying the inhibitory effects of three BNI compounds—1,9-D, MHPP, and LA—on native *N. europaea*. These compounds were selected because their inhibition effects have been reported across multiple studies, facilitating broad comparisons and benchmarking. By determining the half-maximal inhibitory concentrations (IC_{50}) under controlled conditions and assessing the reversibility in inhibition, this study provides critical insights into these BNI compounds and their applications in agriculture.

The objectives of this study were:

a. To determine the IC_{50} values of 1,9-D, MHPP, and LA using native *N. europaea*.
b. To evaluate the reversibility of inhibition for these compounds.

Materials and Methods

General Setup and Culture Conditions

Gen.1a. Bacterial strain and growth conditions

Prior to use, all glassware was washed, soaked in a 0.1% nitric acid bath for at least 2 hours, rinsed twice with deionized (DI) water, and autoclaved. *N. europaea* (ATCC 19718)

cultures were cultivated in ATCC medium 2265 containing 22.5 mM $(NH_4)_2SO_4$, 3 mM KH_2PO_4, 2.18 mM K_2HPO_4, 3.77 mM Na_2CO_3, 750 µM $MgSO_4$, 200 µM $CaCl_2$, 10 µM $FeSO_4$, 16 µM EDTA (free acid), and 0.5 µM $CuSO_4$ (detailed medium recipe in Appendix A). Cultures were maintained in 500 mL volumes within 2 L Erlenmeyer flasks and incubated at 30°C in the dark with continuous shaking at 120 rpm. The flasks were wrapped in foil for additional protection from the light, as *N. europaea* are light-sensitive. Culture purity was verified by plating on nutrient agar, while growth was monitored through optical density at 600 nm (OD_{600}) using an Agilent Technologies Carry 60 UV-Vis Spectrophotometer and NO_2^- concentrations determined by a Griess assay (described below). After 3-days, cultures reached mid-exponential growth with an OD_{600} of approximately 0.07. To achieve a higher OD_{600}, cells at an OD_{600} of 0.05 were centrifuged and resuspended in 500 mL medium, which facilitated continued exponential growth, reaching an OD_{600} ~ 0.1 within approximately 24 hours.

Gen.1b. NO_2^- Quantification

NO_2^- concentrations were determined using a colorimetric assay with the Griess Reagent Kit (Thermo Scientific) on a 96-well microplate. Each reaction well contained 130 µL of deionized (DI) water, 150 µL of sample, and 20 µL of Griess Reagent (equal parts *N*-(1-naphthyl)ethylenediamine dihydrochloride and sulfanilic acid). The mixture was incubated for 30 minutes, during which the reagent develops a colorimetric response: bright magenta at high NO_2^- concentrations and light pink at low NO_2^- concentrations. After the incubation period, absorbance was measured at 548 nm on an Agilent BioTek EPOCH 2 microplate reader. A standard curve was generated using NO_2^- concentrations of 0, 5, 10, 20, 50, and 100 µM. The detection range for the microplate assay was 0-50 µM, thus proper dilution factors were applied

to ensure sample measurements remained within this range. Background NO_2^- was measured at the start of each experiment to establish baseline concentrations.

Gen.1c. Cell harvesting and preparation

Cultures were harvested in mid-exponential growth by centrifugation at 5,000 x *g* (relative centrifugal force, RCF; $g = 9.81\ m/s^2$) for 30 minutes at 4°C. The pelleted cells were decanted, washed with fresh media, and centrifuged again. Harvested cells were resuspended in fresh media and utilized for experiments.

Gen.1d. Chemicals

All chemicals used in media preparation or other experimental procedures were of analytical grade and purchased from Thermo Scientific. Isolated BNI compounds, including 1,9-D, MHPP, and LA, were obtained at the highest available purity (≥ 95%) from Sigma Aldrich (St. Louis, MO), Thermo Scientific (Waltham, MA), and Activate Scientific (Prien am Chiemsee, Germany). Compounds were stored according to manufacturer recommendations, typically at 4°C or 20°C, and protected from light.

Experiment 1: Determination of the Nitrification IC_{50}

This experiment focuses on determining the concentration of a BNI compound that results in 50% inhibition of nitrification (IC_{50}).

Experiment 1a. IC_{50} Assay Setup

This experiment focused on determining the IC_{50} of selected BNI compounds by testing various concentrations on a constant biomass concentration. *N. europaea* cells were grown in batch and harvested as described above. The cells were resuspended in fresh medium to achieve a target OD_{600} concentration in the well, allowing for the assessment of different BNI compound concentrations at the same biomass level. In a 96-well plate, with triplicates per condition, 250

µL of resuspended *N. europaea* was added to 50 µL of DI water and BNI compound mix, resulting in a total well volume of 300 µL with the target OD_{600} value. Various concentrations of four different compounds—AT, 1,9-D, MHPP, and LA—were tested. The concentrations tested were as follows: AT at 0.005, 0.01, 0.05, 0.1, 0.25, and 0.5 µM; 1,9-D at 500, 1000, 2500, and 5000 µM; MHPP at 100, 200, 500, 800, and 1000 µM; and LA at 0.7, 1.4, 2.8, 5.7, and 57 µM. For LA, a concentration of 5.7 µM corresponds to its solubility limit of 1.6 mg/L, while the highest concentration tested, 57 µM, exceeded its solubility, reaching 16 mg/L. All compounds were dissolved in fresh media, except LA, which was dissolved in dimethyl sulfoxide (DMSO) due to its limited solubility. The maximum final DMSO concentration in the well was maintained at or below 0.1% to minimize any potential effects on bacterial activity. An aliquot between 1 µL and 50 µL of the BNI compound stock was added to each well to achieve the desired BNI compound concentration, with the remaining volume filled with DI water to achieve a final well volume of 300 µL. This experiment was repeated at OD_{600} values of 0.1 and 0.015 to determine the impact of biomass concentration on inhibition levels.

Two microplates were prepared: one for the initial NO_2^- measurement (0 h) and one for the final measurement (1 h). The samples were incubated for 1 hour at 30°C in the dark with continuous shaking at 120 rpm. NO_2^- levels were measured at each time point using the Griess Assay, as described in Chapter 2, Gen. 1b. At each time point, 20 µL of the stop solution 0.1 M AT was added to prevent additional NO_2^- from forming in the incubation period for the Griess reagent. Proper dilution factors were applied to ensure sample measurements remained within the assay's detection range. Wells containing *N. europaea* with 50 µL DI water served as controls and references for inhibition calculations.

Experiment 1b. Inhibition Calculation

For each treatment, the NO_2^- concentration at each time point was averaged. Then the net NO_2^- was then calculated using Equation 1.1. Inhibition was determined using Equation 1.2, calculated as a ratio between the treatment's net NO_2^- to that of the control, with the control defined 0% inhibition.

Eq. 1.1:

$$Net\ Nitrite = (NO_2^-)_{final} - (NO_2^-)_{initial}$$

Eq. 1.2:

$$Inhibition\ (\%) = (1 - \frac{Average\ Net\ NO_2^-\ \text{Experimental}}{Average\ Net\ NO_2^-\ \text{Control}}) * 100$$

Experiment 1c. IC_{50} Model

The half-maximal concentration (IC_{50}), representing the inhibitor concentration that reduces NO_2^- production by 50%, was calculated using GraphPad Prism 10 software. This value was calculated by plotting the inhibitor concentration against NO_2^- inhibition. The curve of best fit and standard error was determined with [Inhibitor] vs Response – Variable Slope with the four parametric logistic (Equation 1.3;Motulsky, 2025). In this equation, *Y* represents percent inhibition, while *X* represents the inhibitor concentration in µM. The top and bottom values were constrained to 100 and 0, respectively, as inhibition cannot exceed 100%. However, for LA, these constraints were not applied, as its inhibition did not exceed 30%.

Eq. 1.3:

$$Y = Bottom + \frac{(Top - Bottom)}{(1+\left(\frac{IC_{50}}{X}\right)^{Hillslope})}$$

$$Y = Inhibition\ percentage\ (\%),\ X = Inhibitor\ Concentration\ (\mu M)$$

Experiment 2: Reversibility of Inhibition

This experiment focused on determining if the inhibition was permanent or reversible by monitoring bacterial activity after the removal of BNI compounds.

Experiment 2a. Inhibition Exposure and Initial Monitoring

N. europaea cells were grown in batch and harvested as described above. Initially, the experiment was conducted in a 96-well microplate; however, the wash step to remove the inhibitors proved challenging, so the exposure to inhibitors was carried out in larger volumes. The centrifuged cells were resuspended to a final OD_{600} of 0.1 in 100 mL of fresh medium within acid-washed 500 mL Erlenmeyer flasks. Each flask received one of the following treatments: 0.25 µM AT, 1,500 µM 1,9-D, 425 µM MHPP, or 60 µM LA. These concentrations were selected to elicit inhibition levels ranging from 30% (the maximum inhibition from LA) to 60%, based on preliminary data and previous IC_{50} studies. All compounds were dissolved in DMSO to obtain a final DMSO concentration of 0.1% in the flasks. Flasks without any inhibitors served as the control, and 100 µL DMSO was added to maintain the 0.1% concentration. Flasks were covered in foil and incubated for 2 hours at 30°C in the dark with continuous shaking at 120 rpm. NO_2^- production was monitored every hour utilizing the Griess Assay described in Chapter 2, Gen. 1b.

Experiment 2b. Post-Exposure Monitoring and Reversibility Assessment

After 2 hours of exposure, cells were harvested and centrifuged at 5,000 x *g* (RCF) for 10 minutes at 4°C. Pelleted cells were then washed and centrifuged in fresh medium twice 3,000 x *g* (RCF) for 5 minutes at 20°C. The decrease in time and centrifugal force was to ensure cell viability after centrifugation. The final cell pellet was resuspended with 50 mL of fresh medium and the OD_{600} was measured to ensure a consistent biomass concentration across treatments. If

needed, the OD_{600} was adjusted before distributing the cells into a 96-well microplate, with each well containing 300 µL of resuspended *N. europaea*. NO_2^- production was monitored, following the method outlined earlier, every hour for 2 hours to assess whether the bacterium regained activity once the inhibitors were removed.

Results and Discussion

Bacterial Growth and NO_2^- Production

To validate experimental conditions, the growth of *N. europaea* was monitored using NO_2^- and OD_{600} measurements. NO_2^- concentrations were determined using the standard curve (Figure 2.1). To ensure accurate and reliable measurements, samples were diluted to fall within the linear detection range. NO_2^- accumulation was tracked over time to assess bacterial activity. The steady increase in NO_2^- concentration over the incubation period indicated active NH_4^+ oxidation by *N. europaea*. Maintaining bacterial viability and ensuring consistent nitrification rates were crucial for reliable comparisons and proper evaluation of BNI activity.

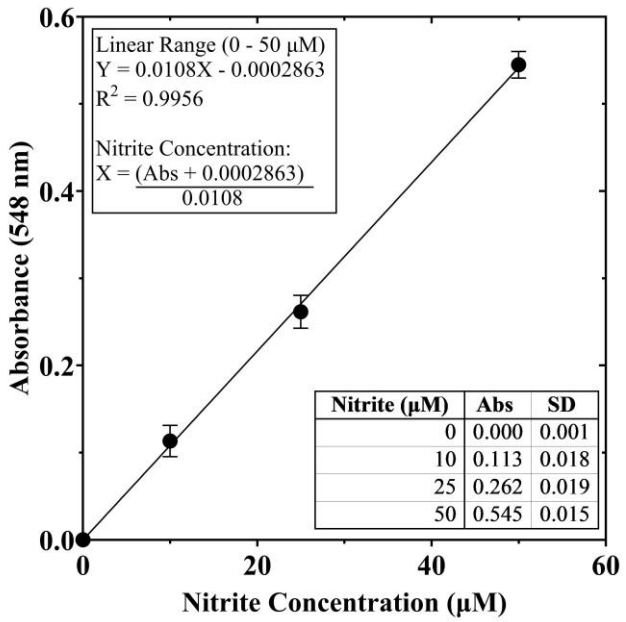

Figure 2.1. Standard curve for NO_2^- quantification.

Sodium nitrite ($NaNO_2$) standards ranging from 0 to 50 µM were prepared in triplicate and reacted with Griess reagents on a 96-well microplate. Absorbance was measured at 548 nm, and the resulting curve was used to interpolate NO_2^- concentration in experimental samples. Error bars represent the standard deviations of triplicate measurements.

In addition to the NO_2^- measurements, the OD_{600} was measured to monitor bacterial growth. The bacterial cultures exhibited consistent growth patterns, reaching the mid-exponential phase within 3 days, with an OD_{600} of 0.07. These results confirmed that the bacterial cultures were stable and capable of sustained nitrification under the experimental conditions.

Determination of IC_{50}

IC_{50} was determined by assessing the effect of BNI compounds on *N. europaea*. The IC_{50} value represents the concentration of the compound required to inhibit nitrification by 50%. To assess this, NO_2^- production was measured during exposure to different concentrations of BNI compounds. A summary is provided below (Table 2.1), followed by a detailed breakdown of each compound's performance.

Table 2.1. Summary of IC_{50} Values

Compound	**OD_{600}**	**IC_{50} (µM) [95% CI Range]**
Allylthiourea (AT)	0.015 0.1	0.15 [0.14 – 0.16] 0.18 [0.15 – 0.22]
1,9-Decanediol (1,9-D)	0.015 0.1	515 [432 - 589] 2,700 [2,100 - 3,500]
Methyl 3-(4-hydroxyphenyl) propionate (MHPP)	0.015 0.1	237 [217 - 258] 368 [301 - 445]
Linoleic Acid (LA)[a]	0.015 0.1	1[a] 60[a]

Note: Values inside the brackets are the IC_{50} values within the 95% confidence interval range. [a]Inhibition for LA did not exceed 30%; thus, the concentration for 10% inhibition (IC_{10}) is reported.

Among the tested compounds, AT and MHPP were the most potent inhibitors, consistently exhibiting low IC_{50} values across biomass concentrations. In contrast, 1,9-D and LA

required significantly higher concentrations to achieve similar inhibition. Notably, 1,9-D displayed the highest variability in IC_{50} across OD_{600} levels, suggesting that its inhibitory effect is strongly influenced by biomass concentration. These differences in potency are closely tied to inhibition patterns, which varied with both compound type and biomass concentration.

Individual Compound Inhibition Profiles

AT: Potent Inhibitor Across Biomass Concentrations

AT demonstrated a nonlinear inhibition in NO_2^- production when native *N. europaea* was exposed to various concentrations (Figure 2.2). This inhibition pattern was observed at both OD_{600} 0.015 and 0.1, indicating that biomass concentration had minimal impact on AT inhibition. The calculated IC_{50} values were 0.15 µM and 0.18 µM for OD_{600} 0.015 and 0.1, respectively, demonstrating that AT remains potent across different biomass levels.

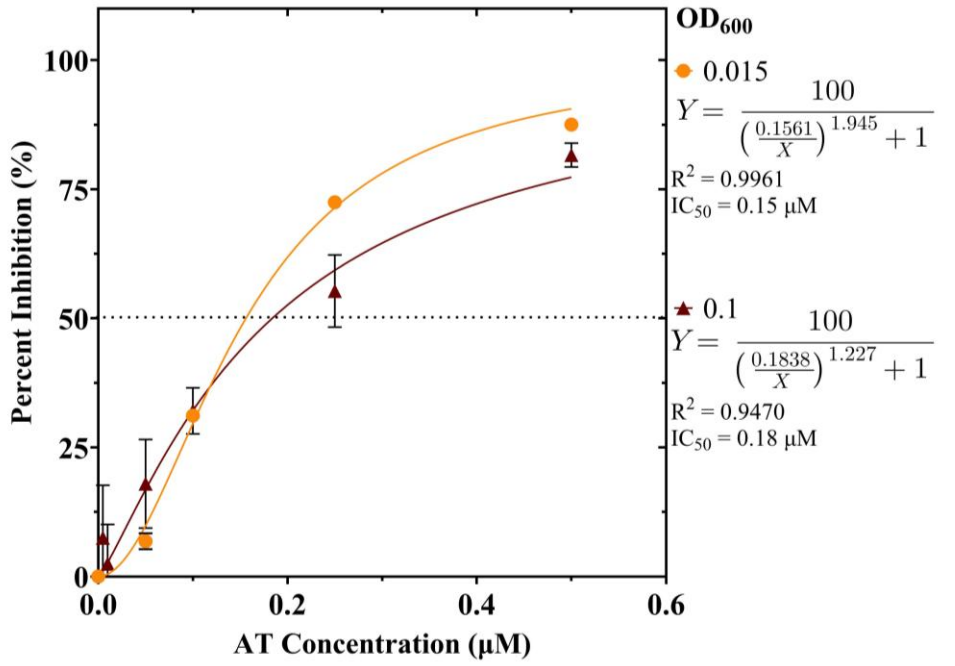

Figure 2.2. Dose-response curves of Allylthiourea (AT) on nitrite production inhibition by *N. europaea* at various OD_{600} values. Inhibition curves reflect *N. europaea* nitrification activity following 1-hour exposure to varying concentrations of Allylthiourea (AT). The percentage of

NO_2^- inhibition was calculated relative to the untreated control. Data points represent the mean ± standard deviation of biological replicates (n = 3). Curves were fitted using a four-parameter logistic model in GraphPad Prism to determine the IC_{50} values.

1,9-D: Biomass-Dependent Inhibitor

1,9-D demonstrated a mixed inhibition pattern, with nonlinear inhibition at OD_{600} 0.015 and linear inhibition at OD_{600} 0.1 (Figure 2.3). The calculated IC_{50} values were 515 µM and 2,700 µM for OD_{600} 0.015 and 0.1, respectively, demonstrating a significant biomass-dependent effect. At lower biomass concentrations, inhibition followed a nonlinear trend, plateauing after a threshold, while at higher biomass concentrations, inhibition became linear.

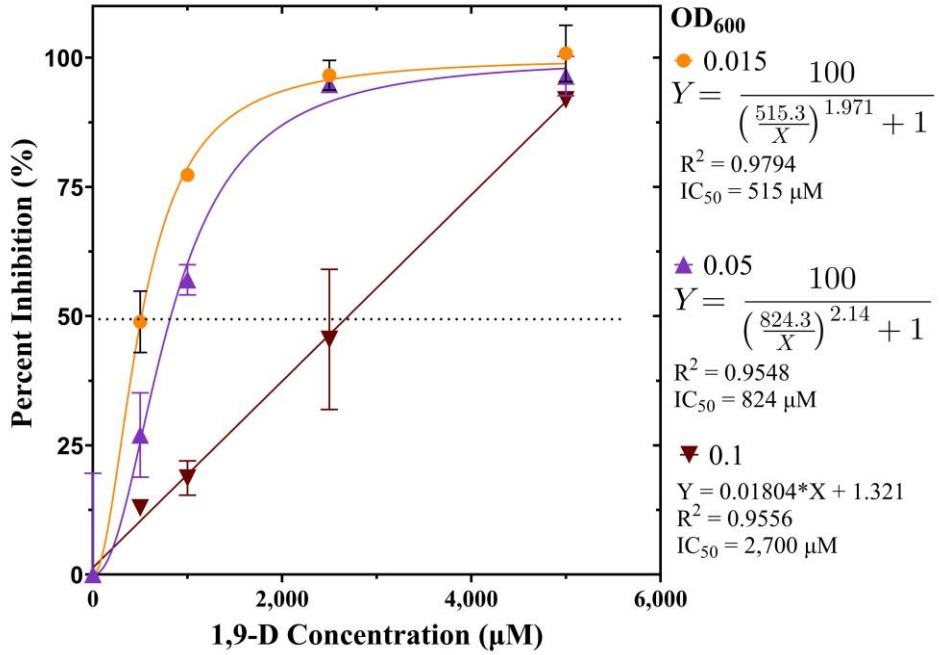

Figure 2.3. Dose-response curves of 1,9-Decanediol (1,9-D) on nitrite production inhibition by *N. europaea* at various OD_{600} values. Inhibition curves reflect *N. europaea* nitrification activity following 1-hour exposure to varying concentrations of 1,9-Decanediol (1,9-D). The percentage of NO_2^- inhibition was calculated relative to the untreated control. Data points

represent the mean ± standard deviation of biological replicates (n = 3). Curves were fitted using a four-parameter logistic model in GraphPad Prism to determine the IC_{50} values.

MHPP: Potent Inhibitor with Minimal Biomass Impact

MHPP demonstrated a nonlinear inhibition in NO_2^- production when native *N. europaea* was exposed to various concentrations (Figure 2.4). The nonlinear inhibition pattern was observed at both OD_{600} 0.015 and 0.1, suggesting that biomass concentration had minimal impact on MHPP inhibition, similar to AT. The calculated IC_{50} values were 237 µM and 368 µM for OD_{600} 0.015 and 0.1, respectively.

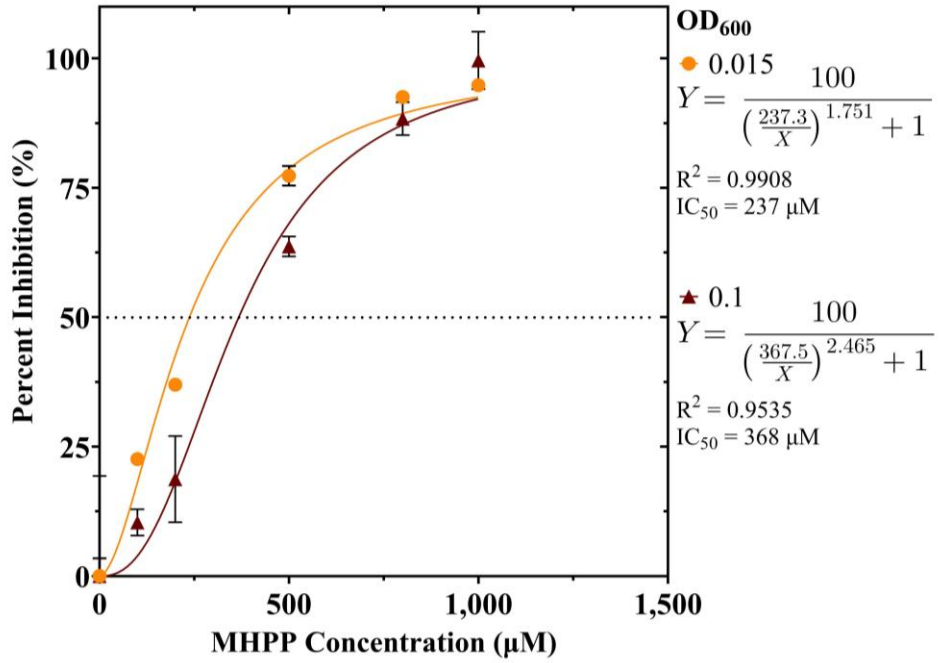

Figure 2.4. Dose-response curves of Methyl 3-(4-hydroxyphenyl) propionate (MHPP) on nitrite production inhibition by *N. europaea* at various OD_{600} values. Inhibition curves reflect *N. europaea* nitrification activity following 1-hour exposure to varying concentrations of Methyl 3-(4-hydroxyphenyl) propionate (MHPP). The percentage of NO_2^- inhibition was calculated relative to the untreated control. Data points represent the mean ± standard deviation of

biological replicates (n = 3). Curves were fitted using a four-parameter logistic model in GraphPad Prism to determine the IC_{50} values.

LA: Ineffective Inhibitor with Low Solubility

LA exhibited nonlinear inhibition at both OD_{600} 0.015 and 0.1, but inhibition did not exceed 30%, making it an ineffective inhibitor compared to other BNI compounds tested (Figure 2.5). Consequently, IC_{10} values (the concentration for 10% inhibition in NO_2^- production) was determined instead of IC_{50} values. The calculated IC_{10} values were 1 µM and 60 µM for OD_{600} 0.015 and 0.1, respectively. It is important to note that LA has extremely low solubility of 1.6 mg/L, even when dissolved in DMSO. Therefore, the 60 µM (16 mg/L) solution exceeded the solubility limit. Despite this, the concentration was tested due to reports of higher usage in previous studies. Subbarao et al. (2008) tested LA at 71 µM (20 µg/mL) and bioluminescent *N. europaea* demonstrated a 95% inhibition in bioluminescence. Thus, a concentration well above solubility limit was included in this study to enable a more comprehensive comparison.

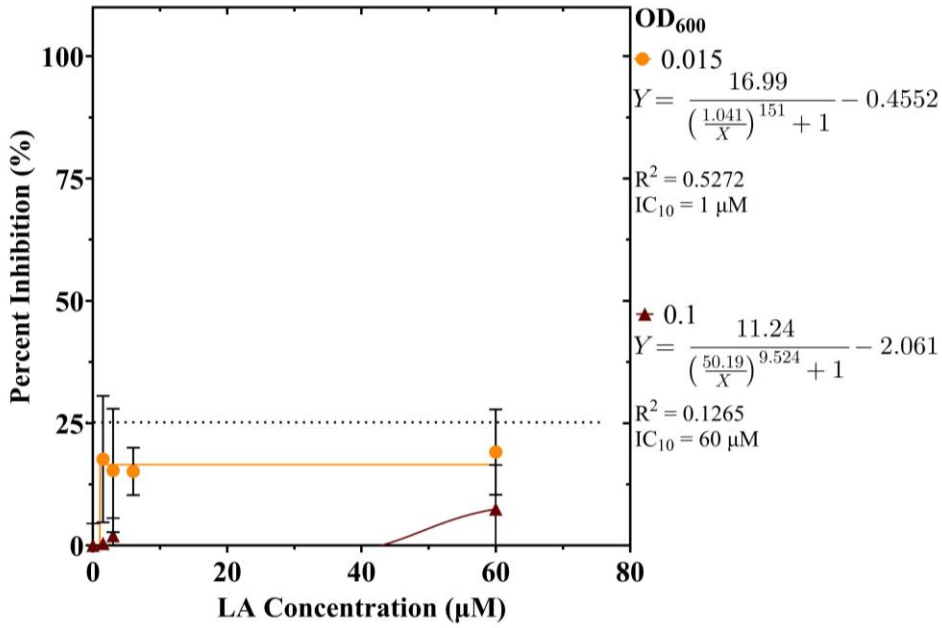

Figure 2.5. Dose-response curves of Linoleic Acid (LA) on nitrite (NO_2^-) production inhibition by *N. europaea* at various OD_{600} values. Inhibition curves reflect *N. europaea* nitrification activity following 1-hour exposure to increasing concentrations of Linoleic Acid (LA). The percentage of NO_2^- inhibition was calculated relative to the untreated control. Data points represent the mean ± standard deviation of biological replicates (n = 3). Curves were fitted using a four-parameter logistic model in GraphPad Prism to determine the IC_{50} values.

Inhibition Patterns

Inhibition patterns observed in this study varied based on both the compound type and biomass concentration. Notably, 1,9-D showed a clear shift from nonlinear inhibition at lower OD_{600} values to linear, dose-dependent inhibition at higher biomass concentrations. This transition suggests a threshold-limited effect at low biomass, where small increases in BNI compound concentration cause steep reductions in activity, followed by a plateau. In contrast, at higher biomass concentrations, inhibition became more linear and predictable, potentially due to increased metabolic capacity and buffering potential of denser cultures (Tarre & Green, 2004). As biomass increases, significantly higher BNI concentrations are required to maintain the same level of inhibition. This interpretation is supported by findings from Tarre & Green (2004), who reported that an increase in biomass concentration was accompanied by a proportional rise in nitrification rate, even under acidic conditions, highlighting the enhanced functional capacity of denser microbial communities. Regardless of the underlying mechanism, biomass concentration appears to plays a significant role in determining the efficacy of BNI compounds.

Additionally, as mentioned earlier, AT and MHPP were the most potent inhibitors, followed by 1,9-D and LA. One key observation is that the IC_{50} values for 1,9-D increased dramatically, from 515 µM at OD_{600} 0.015 to 2,700 µM for OD_{600} 0.1. This sharp increase is

notably larger than the observed increase in MHPP (from 237 µM to 368 µM), suggesting that 1,9-D's inhibitory effect is heavily influenced by changes in biomass concentration. In fact, 1,9-D exhibited the highest variability in IC_{50} values depending on the OD_{600} level, further highlighting its potential dependence on biomass concentration. These findings highlight the importance of standardizing experimental conditions, especially biomass concentration, to ensure accurate comparisons across studies.

Reversibility of Inhibition

The reversibility of inhibition refers to whether a compound's inhibitory effects can be reversed after its removal from the system. Understanding whether inhibition is reversible can offer important insight into the underlying mechanisms of BNIs, which are still under investigation as different compounds may inhibit through distinct pathways. The AMO enzyme can be inhibited either reversibly or irreversibly. Reversible inhibitors form non-covalent interactions with AMO and are generally categorized into two groups: competitive and non-competitive (Bennett et al., 2016; Nardi et al., 2020). Competitive inhibitors bind only to the free enzyme, and since their binding is mutually exclusive with the substrate, they can lead to apparent increases in substrate concentration. Non-competitive inhibitors, on the other hand, can bind to both the enzyme and the enzyme-substrate complex, often causing conformational changes to the enzyme (Bennett et al., 2016; Nardi et al., 2020). For example, AT is a copper-chelating agent and functions as a non-competitive inhibitor, preventing copper from participating in AMO's activity (Nardi et al., 2020; Subbarao, Ito, et al., 2006). Irreversible inhibitors form stable covalent bonds with the active sites of enzymes, permanently deactivating the enzyme. A subset of these, known as suicide inhibitors, mimic the substrate and form covalent bonds with the enzyme that irreversibly inactivate it (Nardi et al., 2020).

While AMO inhibition is a well-documented pathway for nitrification inhibition, it may not be the only mechanism at play. Nitrification can also be influenced by other factors, such as changes in gene expression and membrane disruption (Nardi et al., 2020). Therefore, investigating the reversibility of inhibition is crucial for identifying enzyme-specific interactions and understanding BNI mechanisms further. To assess the reversibility of inhibition, cultures were centrifuged and washed twice to remove residual inhibitor, after which nitrification activity was monitored over time. Inhibition was considered reversible if activity returned to levels comparable to the uninhibited control, suggesting non-permanent, possible competitive binding to AMO (Yildirim et al., 2024). Upon analysis, inhibition by AT, MHPP, 1,9-D, and LA appeared to be largely reversible, as illustrated in Figure 2.6. Notably, cultures previously exposed to 1,9-D exhibited a rapid and complete recovery, regaining 100% nitrification activity within 2 hours of inhibitor removal. Cultures treated with LA and AT also showed substantial recovery. LA cultures reached ~90% recovery approximately 2 hours after washing, while AT cultures started at 50% activity and increased to 95% after 2 hours. In contrast, MHPP exhibited limited recovery (~50%), suggesting a more sustained inhibitory effect. The partial recovery observed in these treatments may reflect temporary metabolic disruption or residual compound effects.

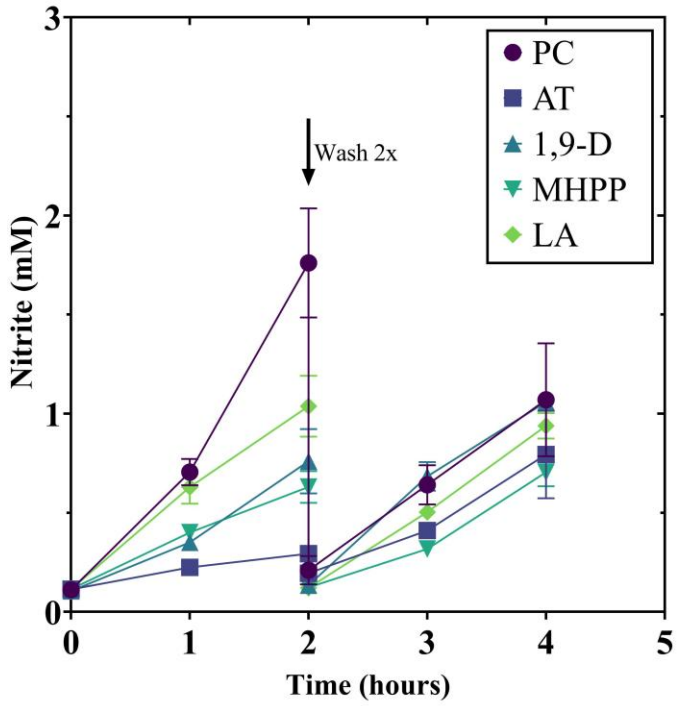

Figure 2.6. Reversibility of Inhibition in *N. europaea* for selected compounds - nitrite production over time. NO_2^- concentrations (mM) were measured during and after a 2-hour exposure to 0.25 µM Allylthiourea (AT), 1,500 µM 1,9-Decanediol (1,9-D), 425 µM Methyl 3-(4-hydroxyphenyl) propionate (MHPP), and 60 µM Linoleic Acid (LA), followed by two wash steps, and a 2-hour recovery monitoring period to assess the reversibility of inhibition. The positive control (PC) served as a baseline for activity. Data were collected from biological replicates (n = 3), and error bars represent the standard deviation.

Overall, the reversibility of inhibition implies that these compounds do not permanently impair nitrifier viability, which is important for understanding their environmental persistence and long-term effects on the soil microbial community. The rapid recovery observed, particularly with 1,9-D, suggests that AOB have the potential to adapt or recover from short-term chemical exposures. The recovery from 1,9-D, AT, and LA suggests reversible inhibition, while the sustained inhibition by MHPP suggests a more persistent effect. These findings emphasize the

need to consider both the immediate and long-term effects of these compounds on soil microbial dynamics and their potential unintended impacts on nutrient cycling.

Comparison with Existing Research

The main motivation behind this study was the discrepancies across previous inhibition studies. These discrepancies can stem from factors such as biological variations, target biomass concentration, and differences in experimental setups. A key distinction in this study was the use of native *N. europaea*, in contrast to the recombinant bioluminescent strain frequently utilized in other studies. Table 2.2 summarizes various studies on the selected compounds, comparing bacterial strains and concentration, and reveals notable differences in IC_{50} values, highlighting the need for a standardized protocol.

Table 2.2. Comparison of IC_{50} values between bioluminescent and native *N. europaea.*

Compound	*N. europaea*	OD_{600}	Value (µM)		Reversible[a]	Reference
AT	Native	0.1	IC_{50}	0.18	Y	This study
	Bioluminescent	7-day[b]	IC_{50}	0.12	NT	Subbarao, Ishikawa, et al. (2006)
1,9-D	Native	0.1	IC_{80}	4,361	Y	This study
		1.0	IC_{80}	516	NT	Sun et al. (2016)
		ND[c]	IC_{20}	440	NT	Kaur-Bhambra et al. (2022)
MHPP	Native	0.1	IC_{50}	403	Y	This study
		ND[c]	IC_{50}	340	NT	Kaur-Bhambra et al. (2022)
	Bioluminescent	7-day[b]	IC_{70}	9	NT	Zakir et al. (2008)
LA	Native	0.1	IC_{10}	60	Y	This study
		ND[c]	IC_{80}	622	NT	Kaur-Bhambra et al. (2022)
	Bioluminescent	7-day[b]	IC_{80}	60	Y	Subbarao et al. (2008)

[a] Y = Yes. NT = Not Tested. [b] 7-day refers to a 7-day culture as the OD_{600} value was not defined in the study. Based on *N. europaea*'s typical growth curve, 7-day samples have an OD_{600} of 0.1 or higher, depending on the growth conditions. [c] ND = Not Defined.

Notably, variation in IC_{50} values was observed between native and bioluminescent strains, emphasizing the influence of strain-specific characteristics on BNI sensitivity. For instance, when comparing results with Subbarao, Ishikawa, et al. (2006), the inhibitory effect of AT was relatively consistent, with IC_{50} values of 0.18 µM (native) and 0.12 µM (bioluminescent). Since AT inhibits AMO, these consistent IC_{50} values suggest comparable AMO expression across both strains. In contrast, MHPP exhibited a dramatic difference between strains. The bioluminescent strain showed high sensitivity (IC_{50} < 9 µM), while the native strain required 45-times higher concentration (IC_{50} = 403 µM). This stark discrepancy may reflect differences in membrane composition or cellular physiology introduced by *luxAB* gene insertion. The integration of *lux* genes may impose a metabolic burden, potentially altering gene expression or stress responses and increasing susceptibility to certain inhibitors (Bazhenov et al., 2023). Understanding how these physiological shifts influence BNI activity is crucial in interpreting strain-specific responses.

Additional differences in MHPP sensitivity were observed within native cultures, potentially driven by biomass concentration. Kaur-Bhambra et al. (2022) reported a slightly lower IC_{50} value of 340 µM at an undefined OD_{600}. Their study spanned one week, with measurements taken twice daily, suggesting that changes in biomass and physiological state over time may have influenced inhibitor sensitivity. While IC_{50} values between native strains are fairly close (403 vs. 340 µM), they remain notably higher than that of the bioluminescent strain, reinforcing the idea that strain type might exert a strong influence on inhibitor response.

Beyond strain-related differences, further insights into the impact of biomass concentration are evident when examining 1,9-D sensitivity. Sun et al. (2016) reported an IC_{80} value for 1,9-D of 516 µM for a 7-day old native culture at an OD_{600} of 1.0 within a 2-hour incubation. This value is substantially lower than the IC_{80} value observed in this study (4,361 µM at OD_{600} = 0.1). In another study, the observed IC_{20} value was 440 µM at an undefined OD_{600}; assuming a continued linear trend, the extrapolated IC_{80} value would be approximately 1,557 µM (Kaur-Bhambra et al., 2022). While this estimate aligns more closely with native strain behavior, it remains significantly lower than the value observed in this study (4,361 µM at OD_{600} = 0.1). These differences could be explained by the higher biomass concentration in Sun et al. (2016), but this result seems counterintuitive. Typically, a higher biomass would require a greater amount of inhibitor; instead, this discrepancy may reflect differences in cellular uptake, nutrient bioavailability, or physiological state of the cells.

In addition to MHPP and 1,9-D, LA presented unique inhibitory patterns across strains. In this study with native cultures, 60 µM LA resulted in only ~30% inhibition, while the bioluminescent strain displayed up to 80% inhibition (Subbarao et al., 2008). This pronounced difference suggests that the bioluminescent strain may be more sensitive to LA, potentially due to the impacts of *lux* gene insertion on bacterial surface properties (Chen et al., 2008), and could respond differently than native strains. Additionally, LA's low solubility may have impacted inhibitory effects. LA is poorly soluble in water (~1.6 mg/L or 5.7 µM), but is highly soluble in DMSO. In this study, LA was initially dissolved in low concentrations of DMSO. Kaur-Bhambra et al. (2022) followed a similar approach, dissolving LA in 100% DMSO and diluting to a final concentration of 0.1% DMSO in the assay. Their study tested LA concentrations up to 750 µM, reporting an IC_{80} value of 622 µM (Kaur-Bhambra et al., 2022). While DMSO improves

dispersal of hydrophobic compounds, LA still likely formed micelles or adsorbed to surfaces once added to the media, especially at concentrations exceeding its solubility limit (Degrand et al., 2023). This aggregation of LA could create a physical barrier to gas exchange, thereby potentially reducing oxygen diffusion in the culture medium, further complicating the interpretation of inhibitory effects. As a result, the actual bioavailable concentration of LA in the medium might be lower than expected, making it difficult to directly compare nominal concentrations across studies or strains.

Despite solubility limitations, several studies have explored how LA exerts its inhibitory effect on microbial systems. Mechanistically, LA has been shown to disrupt microbial membranes. For instance, Lv et al. (2020) reported that LA inhibited *Lactobacillus*, a gram-positive gastrointestinal bacterium, by destroying the cell membrane and affecting cellular metabolism. Similarly, LA was found to inhibit the biofilm formation of *Pseudomonas aeruginosa* on reverse osmosis membranes (Kim et al., 2019). LA may impact AOBs through comparable membrane-targeting mechanisms. However, these results must be interpreted within the context of limited solubility, DMSO effects, and surface properties. Therefore, the observed differences in LA sensitivity likely reflect both strain-specific responses and physicochemical limitations of LA delivery and availability.

Nevertheless, reversibility was suggested in both Subbarao et al. (2008) and the present study. While Subbarao et al. (2008) did not explicitly confirm reversibility, they suggested that LA may not be a suicidal inhibitor. This aligns with the findings of this study, where *N. europaea* cultures regained ammonia oxidation activity upon LA removal. This observed reversibility adds further insight into the complexity of LA's interaction with microbial system and suggests that its effect might be mitigated under certain conditions.

Although specific values varied, one consistent finding across studies is that MHPP demonstrates greater effectiveness than 1,9-D. Sun et al. (2016) reported 1,9-D had a much higher IC_{80} value than MHPP, a trend also observed in this study. Together, these observed differences highlight the complexity of comparing values across studies and emphasize the need for standardized conditions when evaluating BNI compound effectiveness.

Limitations

Several experimental limitations should be considered when interpreting the results of this study. As an obligate aerobic microorganism, the activity of *N. europaea* is influenced by oxygen availability (Arp et al., 2002). One limitation of this study is the use of 96-well microplates, which offer limited headspace and surface area for efficient oxygen transfer. The small headspace (60 µL) and relatively large media volume (300 µL) may restrict oxygen exchange between the air and the liquid phase, potentially leading to lower dissolved oxygen (DO) levels than those observed in open systems. Based on the Henry's constant, the estimated DO concentration in the wells was 2.016 mg O_2/L (see Appendix B for detailed calculations). However, this value should be adjusted to account for the ionic strength in the media, which can affect the solubility of oxygen. Consequently, the actual DO concentration might be slightly lower than estimated due to this influence. Yu & Chandran (2010) demonstrated in a 200-hour experiment that under low dissolved oxygen (DO) concentrations, the conversion of NH_4^+ to NO_2^- was significantly reduced—76% conversion at DO = 0.5 mg O_2/L and a 90% conversion at DO = 1.5 mg O_2/L. However, the maximum specific growth rates were not statistically impacted over this period, suggesting that while oxygen availability influences substrate conversion, it may not strongly affect growth kinetics in the short term. That said, their experiment spanned 200 hours, whereas the current study only observed activity over 1 hour, so the impact of oxygen

limitations may be negligible. Still, even within shorter exposure periods, reduced oxygen availability may influence nitrification activity, and consequently, may impact the observed inhibition (R. Yu & Chandran, 2010). However, this constraint may still reflect realistic conditions in soil environments, where oxygen availability is often limited depending on the soil type and conditions. Another limitation of this study is the reliance on OD_{600} as a proxy for biomass concentration. While OD_{600} provides a convenient and rapid estimate, it does not account for differences in cell viability, metabolic state, or cell clusters, which may influence inhibition dynamics.

Additionally, compound solubility posed a challenge, particularly for LA, which exceeded its solubility limit at higher concentrations. This could lead to an underestimation of inhibitory effects or inconsistent exposure levels. Furthermore, the inhibition observed may have been influenced by compound degradation or transformation over time. Without analytical verification of compound stability, it is difficult to determine whether the observed inhibition can be attributed solely to the inhibitor's presence. Lastly, while *N. europaea* serves as a well-established model organism for nitrification, these results may not fully capture the complexity of nitrifying communities in natural soil, particularly in the rhizosphere, where diverse interactions and competitive processes occur. Future studies should aim to explore the dynamics of these complex microbial communities to better understand how BNIs affect nitrification in a more ecological setting.

Future Research

Further research could help expand and refine the findings of this study. One valuable direction would be to monitor additional N forms, such as NH_4^+ and N_2O, to gain a more comprehensive understanding of how BNI compounds influence the full nitrification pathway.

Including these metrics would provide insights in shifts of N transformation and GHG emissions. Future studies could explore a broader range of OD_{600} values to better characterize the biomass-dependent effects of compounds like MHPP. This may help identify a clear linear range and threshold value for these compounds. In addition, evaluating the long-term stability of BNI compounds and their degradation products could offer clarity on their persistence and potential for sustained inhibition. Finally, incorporating diverse microbial communities or soil microcosms would provide a more realistic representation of environmental conditions, allowing for validation of laboratory findings under more complex scenarios. This approach would also provide insight into the broader ecological impact of BNI compounds on soil microbial communities. Future research would enhance the application of BNI compounds in agricultural systems by optimizing concentration strategies for effective nitrification management.

Conclusions

This study highlights the variability in nitrification inhibition patterns among different BNI compounds and the significant role the biomass concentration plays in shaping these responses. Compounds such as AT and MHPP consistently demonstrated consistent IC_{50} values across biomass levels, while 1,9-D and LA required much higher concentrations to achieve comparable levels. Notably, 1,9-D exhibited the most pronounced biomass-dependent inhibition, with IC_{50} values increasing more than five-fold between low and high OD_{600}. These trends suggest that inhibition mechanisms are closely linked to microbial density, metabolic buffering, and compound interactions within the culture environment. Consequently, it is crucial to standardize the biomass concentration to ensure reproducibility and cross-study comparisons. Regarding reversibility, 1,9-D showed complete recovery potential, with cultures regaining 100% activity within 2 hours of its removal. While AT, MHPP, and LA were also reversible,

they caused a temporary reduction in nitrification rates following removal, indicating residual metabolic disruption rather than permanent damage. Overall, the distinct inhibition profiles of each compound emphasize the need for continued research into the behavior of these compounds within soil ecosystems. This study contributes to the deeper understanding of BNI compounds, their physiological impact on *N. europaea*, and the mechanisms underlying their inhibition.

Chapter 3 - Transcriptomic Response of *N. europaea* Upon Exposure to BNI Compounds

Abstract

AOBs, such as *N. europaea*, catalyze the first step of nitrification, converting NH_4^+ to NO_2^-. *N. europaea* is one of the most well-characterized AOBs, with its complete genome sequenced, making it a model organism for studying nitrification. Exposure to BNI compounds has a significant impact on the physiology of *N. europaea*, particularly by reducing NO_2^- production. In this study, whole-genome transcriptomics were employed to investigate the gene expression and regulatory changes in *N. europaea* upon exposure to three BNI compounds—1,9-D, MHPP, and LA—with AT as a reference inhibitor. Preliminary RNA extraction and quantitative polymerase chain reaction (qPCR) analysis revealed a corresponding inhibition in both NO_2^- production and expression of the *amoA* gene, which encodes a key enzyme, AMO, involved in nitrification. Together, these results demonstrate that BNI compounds suppress key genes in the nitrification pathway and offer new insight into the molecular mechanisms underlying BNI.

Introduction

In addition to quantifying and identifying the physiological impacts, it is important to explore the underlying genetic and molecular responses of *N. europaea* to these compounds. These compounds were selected to ensure consistency throughout this thesis and because their mode of inhibition have been reported across multiple studies. AT, 1,9-D, and MHPP disrupt the activity of AMO, while LA inhibits both AMO and HAO (Subbarao et al., 2008; Sun et al., 2016; Zakir et al., 2008). This variation in mode of inhibition provides a more comprehensive

understanding of how different inhibitors affect nitrification pathways and corresponding gene expression. Investigating the transcriptional response of *N. europaea* to these compounds can deepen our understanding of nitrification regulation and support the development of targeted, sustainable strategies in agriculture.

Overview of Gene Expression and Ribonucleic Acid (RNA)

Deoxyribonucleic acid (DNA) and ribonucleic acid (RNA) are essential molecules that carry and express genetic information. Genes, composed of DNA, are the functional units that encode for proteins, cell structures, and specific biochemical functions (Actor, 2012). Gene expression occurs through a two-step molecular process: transcription and translation. During transcription, DNA is transcribed into messenger RNA (mRNA), a class of RNA that carries genetic instructions from the genome to the ribosomes. In translation, ribosomes read the mRNA sequence and synthesize the corresponding proteins, including enzymes responsible for cellular metabolism and function (Actor, 2012). In response to environmental stress, such as chemical exposure, nutrient limitations, or inhibitors, cells can rapidly adjust their gene expression (Clark et al., 2019). This often involves upregulation or downregulation of specific genes, enabling a quick genetic response to changing conditions.

Genes Associated with Nitrification

As previously discussed, *N. europaea* plays a pivotal role in the N cycle by mediating nitrification. This process is driven by two key enzymes, AMO and HAO (Kowalchuk & Stephen, 2001; Li et al., 2022); however, this study specifically focuses on AMO, as it catalyzes the first and rate-limiting step of nitrification. The AMO enzyme is encoded by three genes—*amoC*, *amoA*, and *amoB*—organized in the *amoCAB* operon. Notably, *N. europaea* contains two full copies of this operon in its genome (Stein et al., 2000). Of these genes, the *amoA* gene

encodes the subunit of AMO that contains the enzyme's active site, making it crucial for AMO function. In this study, *amoA* is used as a molecular marker to assess the transcriptional impact of BNI compounds on *N. europaea*. Changes in *amoA* expression serve as an indicator of the organism's response at the genetic level.

The objectives of this study were:

a. To determine the optimal sampling time for RNA extraction from native *N. europaea*.
b. To analyze the transcriptomic response of native *N. europaea* upon exposure to BNI compounds.

Materials and Methods

General Setup and Culture Conditions

The general experimental setup and culture conditions for the following experiments are identical to those described in Chapter 2, General Setup. However, centrifugation was conducted for 10 minutes, not 30 minutes, to assist in sample collection and reduce the impact of centrifugation on RNA.

Experiment 1: Preliminary Timing for RNA Extraction

Experiment 1a. Incubation Setup

N. europaea cells were grown in batch and harvested as described above in Chapter 2, General Setup. The cells were resuspended to a final OD_{600} of 0.1 in 100 mL of fresh medium within 500 mL Erlenmeyer flasks. However, for LA, the target OD_{600} was 0.015 to enhance the observable inhibition, as higher biomass (OD_{600} = 0.1) reduced sensitivity in prior IC_{50} experiments. The criteria used to select the proper BNI compound concentrations for RNA sequencing was to cause a significant change in cell physiology without being too damaging to

vital cell processes. Thus, 50%-90% inhibition in NO_2^- production was determined to be the desired level of inhibition for this study. Each flask contained one of the following treatments in triplicates: 0.5 µM AT, 1,500 µM 1,9-D, 425 µM MHPP, or 60 µM LA. These compounds were dissolved in DMSO to obtain a final DMSO concentration of 0.1%. Flasks without any BNI compound served as the control, and 100 µL DMSO were added to maintain 0.1%. Flasks were covered in foil and incubated for 24 hours at 30°C in the dark with continuous shaking at 120 rpm.

NO_2^- production was monitored at 0 h, 1 h, 3 h, 5 h, 10 h, and 24 h to determine the optimal time for RNA extraction. At each time point, a 5 mL sample from each flask was collected and centrifuged at 5,000 x *g* (RCF) for 10 minutes at 4°C. Pellets were resuspended in 1 mL of RNAProtect (QIAGEN) and stored at -80°C until extraction.

Experiment 1b. RNA Extraction

RNA extraction was conducted by Seongmin Yang, Ph.D Candidate in Civil Engineering, at Kansas State University. The KingFisher™ Duo Prime Purification System (Thermo Scientific™) was used to extract DNA, which can process 12 samples in one run. Samples and reagents were prepared and pipetted in a standard KingFisher™ deep-well 96-well plate following the instructions provided with the DNA extraction kit. The MagMAX_Microbiome_Liquid_Buccal_Duo protocol was selected for the purification. Purified DNA obtained in elution strips were transferred into new Eppendorf strips and were stored at 4°C temporarily until concentrations were measured as required for further experiments, before storing at -80°C.

Following DNA extraction, total RNA was isolated from the same samples using the same KingFisher™ Duo Prime Purification System (Thermo Scientific™) with RNA-specific

reagents and protocols. The extracted RNA was then treated with EZ DNAse (Invitrogen) to remove any residual genomic DNA. Subsequently, complementary DNA (cDNA) was synthesized using SuperScript™ IV Reverse Transcriptase (Thermo Fisher Scientific) according to the manufacturer's protocol. The resulting cDNA was stored at -20°C until further use in qPCR analysis.

Experiment 1c. Quantitative Polymerase Chain Reaction (qPCR) Analysis

Polymerase Chain Reaction (PCR) was conducted with universal 16S rRNA gene primers on DNase-treated RNA samples to confirm the absence of DNA contamination. Target genes and transcripts were quantified by qPCR using a CFX Opus 96 Real Time PCR System (Bio-Rad, Hercules, CA, USA) in 20 µL reaction mixtures containing 10 µL of SsoAdvanced™ Universal SYBR Green Supermix (Bio-Rad, Hercules, CA, USA), 300 nM of each primer, and 2 µL of template DNA. Quantification was performed using standard curves prepared from serial 10-fold dilutions of cloned plasmids or double-stranded synthetic DNA fragments (gBlocks®, Integrated DNA Technologies, Coralville, IA, USA) in triplicate. Detailed information on primer sequences, standard sequences, and detection limits can be found in Appendix C.

Experiment 2: Final RNA Extraction and Transcriptome Sequencing

Experiment 2a. Incubation and Sampling

Experiment 2 followed the same cultivation and treatment setup as Experiment 2, using the same BNI concentrations and flask conditions. However, the incubation times were shortened based on preliminary results from Experiment 1. Flasks were incubated for 3 hours (AT, 1,9-D, and MHPP) or 5 hours (LA) at 30°C in the dark with continuous shaking at 120 rpm. NO_2^- production was monitored initially and at the final sampling. After incubation, the entire 100 mL culture from each flask was collected and centrifuged at 5,000 x *g* (RCF) for 10 minutes at 4°C.

Pellets were resuspended in 1 mL of RNAProtect (QIAGEN) and stored at -80°C until RNA extraction.

Experiment 2b. RNA Extraction

RNA extraction was performed as described in Experiment 1b using the KingFisher™ Duo Prime Purification System (Thermo Scientific™).

Experiment 2c. Quantitative Polymerase Chain Reaction (qPCR) Analysis

qPCR analysis was conducted as outlined in Experiment 1c to verify transcript abundance and support RNA sequencing results.

Experiment 2d. RNA Sequencing and Annotation

RNA samples were sent to Novogene for transcriptome sequencing. Subsequent annotation and analysis will be conducted at the K-State Integrated Genomics Facility.

Results and Discussion

Physiological Responses to BNI Compounds

While the focus of this chapter is on the transcriptomic response to BNI, it is important to first validate the physiological impacts to contextualize the corresponding changes in gene expression. In terms of NO_2^- production, all tested BNI compounds exhibited significant inhibition. AT resulted in an average inhibition of 85%, 1,9-D at 63%, and MHPP at 76% (Figure 3.1). LA was the lowest at 19%, which was expected given that its maximum inhibitory effect of 30% was observed at 60 µM earlier in the study.

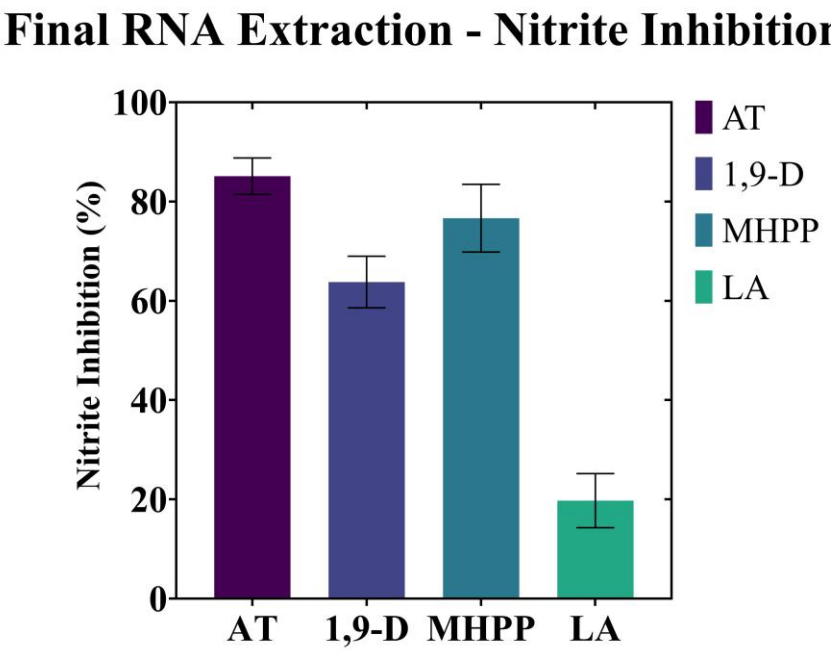

Figure 3.1. Nitrite Inhibition in RNA Extraction Sample. NO_2^- production inhibition following treatment with 0.5 µM Allylthiourea (AT), 1,500 µM 1,9-Decanediol (1,9-D), 425 µM Methyl 3-(4-hydroxyphenyl) propionate (MHPP), and 60 µM Linoleic Acid (LA). AT, 1,9-D, and MHPP were incubated for 3 hours, while LA was incubated at 5 hours. Data were collected from biological replicates (n = 3), and error bars represent the standard deviation.

Transcriptional Responses to BNI Compounds

qPCR data for *amoA* gene expression was normalized with 16S rRNA gene levels to account for differences in biomass across samples. The normalized *amoA* expression in the positive control (PC) averaged between 0.035 and 0.04, with the PC for AT showing the most variation. These PCs serve as a baseline for comparison with BNI-treated conditions. Preliminary data revealed various responses to the inhibitors, with some treatments showing a significant decrease in *amoA*/16S levels and others showing an increase in *amoA*/16S levels (Figure 3.2). Notably, 1,9-D and MHPP exhibited the most pronounced decrease in *amoA*/16S levels, suggesting a strong transcriptomic response and impact on AMO. In contrast, the AT-treated

sample exhibited substantial variability in *amoA*/16S levels, suggesting potential issues with sample collection and RNA extraction. Additionally, the LA treatment did not significantly inhibit nitrification, which is consistent with the *amoA*/16S ratio remaining comparable to the positive control.

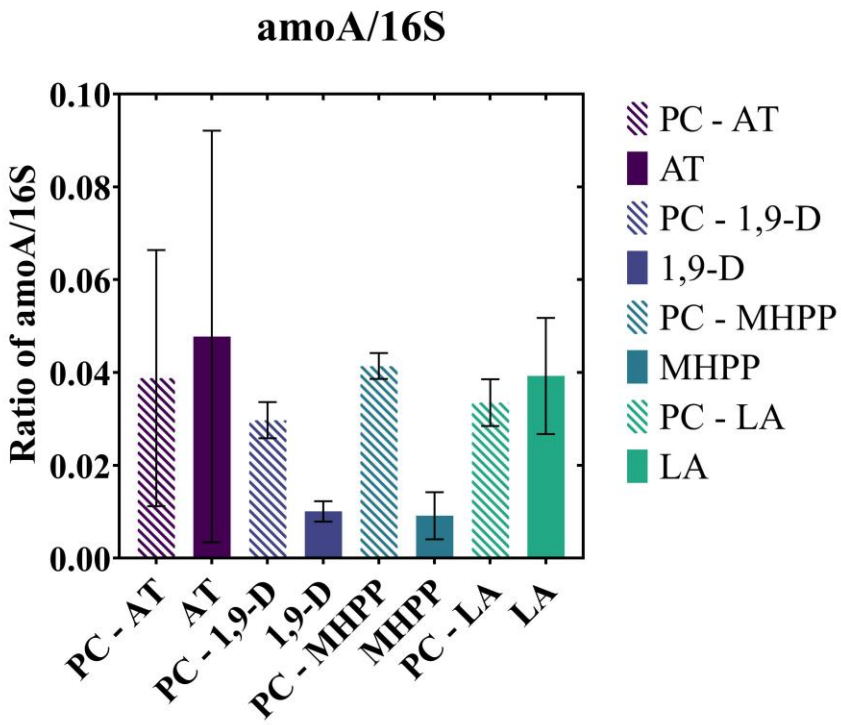

Figure 3.2. *amoA*/16S Ratio in RNA Extraction Sample. The *amoA* gene copy number was normalized to the 16S rRNA gene to assess to potential impact on transcription upon exposure to 0.5 µM Allylthiourea (AT), 1,500 µM 1,9-Decanediol (1,9-D), 425 µM Methyl 3-(4-hydroxyphenyl) propionate (MHPP), and 60 µM Linoleic Acid (LA). Each inhibitor had a corresponding positive control (PC). Data were collected in biological replicates (n=3), and error bars represent the standard deviation.

RNA sequencing was performed by Novogene (Durham, NC) and annotation was conducted at the K-State Integrated Genomics Facility (Manhattan, KS). However, due to processing timelines, the transcriptomic data was not be available for inclusion in this thesis. The

results are expected at a later date and will be analyzed in future work to evaluate the differential gene expression in response to BNI treatments.

Hypothesized Impact of Inhibitors on Gene Expression

Although RNA sequencing data from Novogene is not yet available for inclusion in this thesis, several outcomes can be hypothesized based on previous literature and the experimental design. Based on previous studies and preliminary data, it is expected that inhibitor treatments impacting nitrification, such as 1,9-D and MHPP, will cause significant transcriptional changes in *N. europaea*. Specifically, the downregulation of key nitrification genes, including the *amoCAB* operon (encoding AMO) and *haoBA* (encoding HAO), is anticipated (Sedlacek et al., 2020). Additionally, election transport related genes like *cycB* (cytochrome c552), may also be downregulated as the cells attempt to conserve energy under inhibited conditions (Sedlacek et al., 2020). This predicted response comes from Sedlacek et al. (2020), who reported up to a 3.3-fold decrease in *amoCAB* transcripts under O_2-limited conditions. Stress from inhibitors could also reduce transcription of oxidative stress defense genes, including superoxide dismutase, catalase, peroxidases, and thioredoxins, as the cells shift their priorities toward basic survival. However, certain stress-associated genes, such as rubredoxin (*NE1426*) and a glutaredoxin family protein gene (*NE2328*), were upregulated under O_2-limited conditions in Sedlacek's study, suggesting that select stress responses may be activated depending on the type of environmental pressure. Similarly, exposure to benzene led *N. europaea* to the upregulation of genes associated with lipid biosynthesis and membrane repair (Radniecki et al., 2008), indicating that inhibitor-induced membrane or metabolic stress could also trigger transcriptional activation of efflux pumps, detoxification proteins, or membrane repair pathways. In treatments like AT and LA, where amoA inhibition was not significant, the transcriptional pathways may involve

subtler changes, with potential upregulation of stress responses or energy conservation mechanisms rather than direct suppression of nitrification genes. Inhibitors that strongly disrupt nitrification are expected to downregulate core nitrification pathways while upregulating genes for stress responses.

Given the complex interactions between AOBs and environmental stressors, the detailed analysis of the transcriptomic data will provide insights into the regulatory mechanisms employed by *N. europaea* when exposed to these inhibitors. Additionally, the sequenced transcriptomes will be compared across BNI treatments to identify differentially expressed genes and enriched pathways. Further experiments and analyses will be necessary to validate these hypotheses and provide a comprehensive understanding of the transcriptional shifts associated with nitrification inhibition.

Conclusions

Exposure to BNI compounds results in a genetic response from *N. europaea*, particularly in the expression of the *amoA* gene. For 1,9-D and MHPP, exposure resulted in a significant decrease in *amoA* transcript levels, corresponding to nitrification inhibition rates of 63 and 76%, respectively. This suggests that upon exposure to these inhibitors, the transcriptional pathway for *amoA* is disrupted—likely downregulated as part of the cellular response to stress or inhibited function of the AMO enzyme complex. Further analysis of RNA sequencing data and gene annotations will be crucial in identifying the precise mechanisms behind these transcriptional shifts and providing a more comprehensive understanding of the cellular adaptations to nitrification inhibition. This data will not only confirm the involvement of specific genes but also potentially identify new pathways that could be targeted for future nitrification control.

Chapter 4 - Screening Maize Cultivars for Biological Nitrification Inhibition Activity

Abstract

Low NUE in agricultural systems poses significant economic and environmental challenges; however, BNI offers a promising solution. While BNI activity has been well-documented in various crops like sorghum and rice, the potential for maize (*Zea mays*) to exhibit BNI activity remains under investigation. Recent studies have isolated several BNI compounds from maize roots, including 2,7-dimethoxy-1,4-naphthoquinone (Zeanone), 2-hydroxy-7-methoxy-2*H*-1,4-benzoxazin-3(4*H*)-one (HMBOA), and 6-methoxy-2(3*H*)-benzoxazolone (MBOA) in the *Zea mays* cv Honey Bantam (Otaka et al., 2022, 2023). However, these studies primarily employed recombinant bioluminescent *N. europaea* and filter-evaporated root exudate solutions, which may not fully replicate natural conditions. In contrast, this study aimed to develop an efficient, reproducible, and high-throughput screening method to detect BNI activity in maize root exudates using native *N. europaea*, offering a more realistic assessment of BNI potential in maize cultivars. Several methodological optimizations were implemented, including transitioning from 50-mL flasks to 96-well microplate format, incorporating a stop solution to halt NO_2^- accumulation, adjusting biomass concentration for consistency, and adding a wash step to reduce background NO_2^- levels. Additionally, maize cultivation was shifted to a larger hydroponic system to facilitate root exudate collection and provide large quantities of root mass. The optimized screening protocol significantly improved efficiency, reproducibility, and sensitivity in detecting BNI activity. Several maize cultivars were identified as having BNI

activity, which can help inform breeding strategies and agronomic practices aimed at enhancing NUE and reducing N losses in agricultural systems.

Introduction

As the global population continues to rise, agricultural systems face immense pressure to increase food production to meet the global demand while minimizing environmental impacts. BNI offers a promising strategy to enhance NUE and support more sustainable food systems.

Maize Growth Stages and N Demand

Maize (*Zea mays*) is one of the most widely cultivated crops in the world, especially within the U.S. Midwest region accounting for 20% of global maize production and 60% of U.S. maize production (Goodkind et al., 2023). As a staple crop for global food security, achieving high yields requires effective nutrient management, particularly N management. Understanding maize's nutrient needs across its growth stages is essential for optimizing yields.

Maize undergoes two main growth phases: the vegetative phase, when the plant establishes its leaves, roots, and stalk, and the reproductive phase, when it produces ears and seeds. Within both of these phases there are several stages, labeled as V (vegetative) and R (reproductive), progressing from emergence (VE) to physiological maturity (R6), as illustrated in Figure 4.1. Each stage has distinct water and nutrient requirements, with N demand peaking during vegetative growth and early grain filling, when the plant rapidly accumulates biomass and prepares for reproduction (Ciampitti et al., 2016). Rapid nutrient uptake begins at sixth-leaf stage (V6) and reaches its maximum at silking (R1).

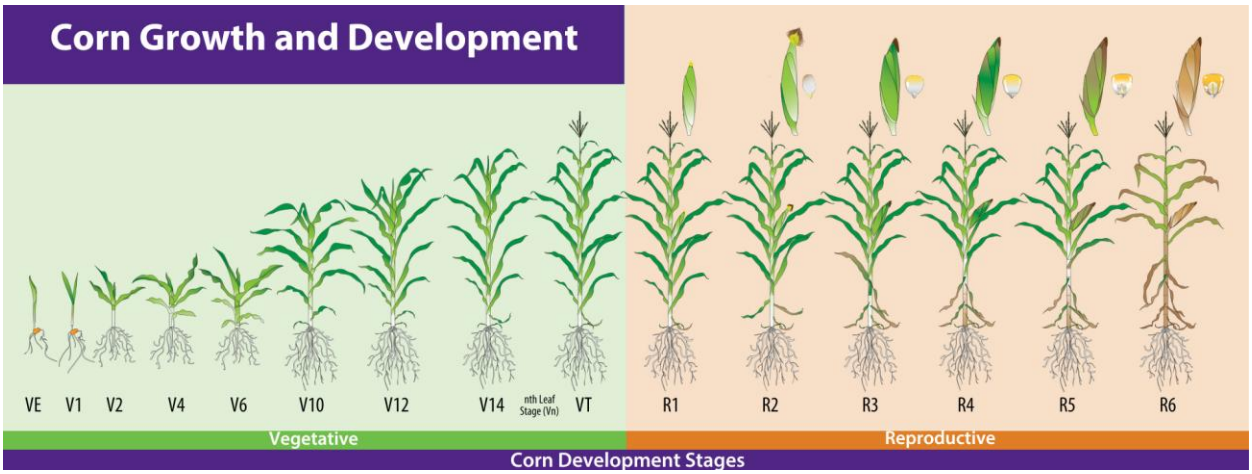

Figure 4.1. Corn Growth and Development (Ciampitti et al., 2016)**.** A visual representation of the key stages in corn growth, beginning with emergence (VE) and ending with physiological maturity (R6).

To meet this nutrient demand, farmers apply substantial amounts of N fertilizer, a practice that supports high yield but also increases production costs and contributes to N losses through leaching and denitrification. Maize is a particularly N-intensive crop, with U.S. farmers applying approximately 12.3 billion pounds (lbs) of N in fertilizer annually—an average of 150 lbs per acre (USDA, 2021). This application rate far exceeds that of other essential nutrients such as phosphate (64 lbs/acre), potash (77 lbs/acre), and sulfur (19 lbs/acre) (Boline, 2024). Fertilizer use accounts for a significant portion of total maize production expenses, representing 17-24% of total costs, or approximately $186.73 per acre in 2023 (Boline, 2024). Unfortunately, much of the applied N is lost, resulting in a NUE of less than 50% (Goodkind et al., 2023), essentially washing farmers' investments away.

BNI Potential in Maize

Given these losses, harnessing BNI potential in maize could provide substantial environmental and economic benefits. Early studies suggested that maize (*Zea mays* var. *Peter 610*)—a botanical variety, i.e. a naturally occurring subgroup within a species—lacked BNI

activity (Subbarao et al., 2007). However, more recent studies have identified genetic markers associated with BNI capacity in several CML inbred lines (Petroli et al., 2023); these elite lines, developed by CIMMYT (International Maize and Wheat Improvement Center), are utilized in both tropical and temperate hybrid-breeding programs (*Maize – CIMMYT*, 2025). Additionally, Otaka et al. (2022) isolated several BNI compounds from maize roots in *Zea mays* cv 'Honey Bantam'—a human-selected cultivar maintained for distinct traits—suggesting that certain maize cultivars may possess the ability to suppress nitrification. Therefore, it is crucial to screen a wide variety of maize cultivars to ensure the full spectrum of BNI activity is captured and the most promising high-BNI cultivars are identified for further development.

BNI Capacity and Success in Wheat

Research in wheat provides an encouraging precedent: Subbarao et al. (2021) discovered that wild wheatgrass (*Leymus mollis*) exhibits strong BNI capacity, mapped the responsible chromosomal region, and successfully transferred the trait into elite wheat varieties. Importantly, transferring this BNI trait did not reduce wheat yield, and in fact enhanced overall N uptake efficiency under field conditions. This demonstration of stable BNI expression in a globally significant cereal crop highlights the feasibility and agronomic value of breeding BNI traits into staple grains like maize.

However, the protocol used to screen for BNI activity was laborious and resource-intensive: root exudate samples were first concentrated via rotary-evaporation, extracted with methanol, reconcentrated, then re-extracted with dimethyl-sulfoxide (DMSO), and finally assayed for BNI using recombinant bioluminescent *N. europaea* (Subbarao et al., 2021). This success story underscores both the promise of BNI breeding and the need for a faster, more scalable screening protocol—precisely the gap this current study seeks to address.

Our Screening Protocol

Our collaborator at the K-State Horticulture and Natural Resources Department has secured 100 different maize germplasms and we have developed a BNI screening protocol using native *N. europaea*. To harness this potential and develop BNI-enhanced crop varieties, it is crucial to establish an efficient method for screening BNI activity. Existing methods—vacuum-evaporation of root exudates followed by sequential methanol and DMSO extractions—are laborious and slow (O'Sullivan et al., 2017; Subbarao et al., 2013). This study aims to streamline the screening process and identify high-BNI cultivars to advance research on the underlying biochemical and genetic mechanisms regulating BNI production. This understanding will ultimately support breeding strategies and agronomic practices aimed at improving NUE in maize production.

The objectives of this study were:

a. To optimize the screening protocol using native *N. europaea* to detect, quantify, and characterize BNI activity released by plant roots.
b. To evaluate the nitrification inhibitory potential of root exudate from different maize cultivars.

Materials and Methods

General Setup and Culture Conditions

The general experimental setup and culture conditions for the following experiments are identical to those described in Chapter 2, General Setup.

Experiment 1: Protocol Optimization for BNI Screening

The protocol for screening BNI activity in maize cultivars underwent several iterations to improve efficiency and reproducibility. Both the growth conditions of maize cultivars and the

screening methodologies evolved over time. Early methods were resource- and time-intensive, prompting modifications to streamline sample handling and improve data accuracy. Protocol modifications included transitioning from 50-mL flasks to a 96-well microplate, addition of a wash step, addition of a stop solution, adjusting the target optical density, and upgrading to a larger hydroponic system. These refinements aimed to increase throughput, reduce variability, and optimize the overall screening process.

Experiment 1a. Initial Experimental Setup

In partnership with Dr. Sunghun Park's lab in the Horticulture and Natural Resources Department at K-State (Manhattan, KS), various maize cultivars were germinated and maintained in a sterile system for BNI screening. The setup for this experiment was adapted from Otaka et al. (2023). To begin, seeds of various maize cultivars were germinated in Root riot cube plugs (Hydrodynamics^{TM}) made of sphagnum peat moss, for 7-10 days depending on the cultivar.

Following germination, the seedlings were transferred to a small-scale hydroponic scaffold system. The roots of the seed were soaked in 50 mL of nutrient medium containing the following: 281 μM KH_2PO_4, 178 μM K_2SO_4, 71 μM $CaCl_2 \cdot 2H_2O$, 150 μM $MgSO_4 \cdot 7H_2O$, 41 μM Fe-EDTA, 922 μM H_3BO_3, 0.3 μM $CuSO_4 \cdot 5H_2O$, 9.1 μM $MnSO_4 \cdot 6H_2O$, 5.2 μM $Na_2MoO_4 \cdot 2H_2O$, and 7.7 μM $ZnSO_4 \cdot 7H_2O$ dissolved in 100 L of DI water. The top of the seed was also covered in a 50-mL tube to prevent contamination.

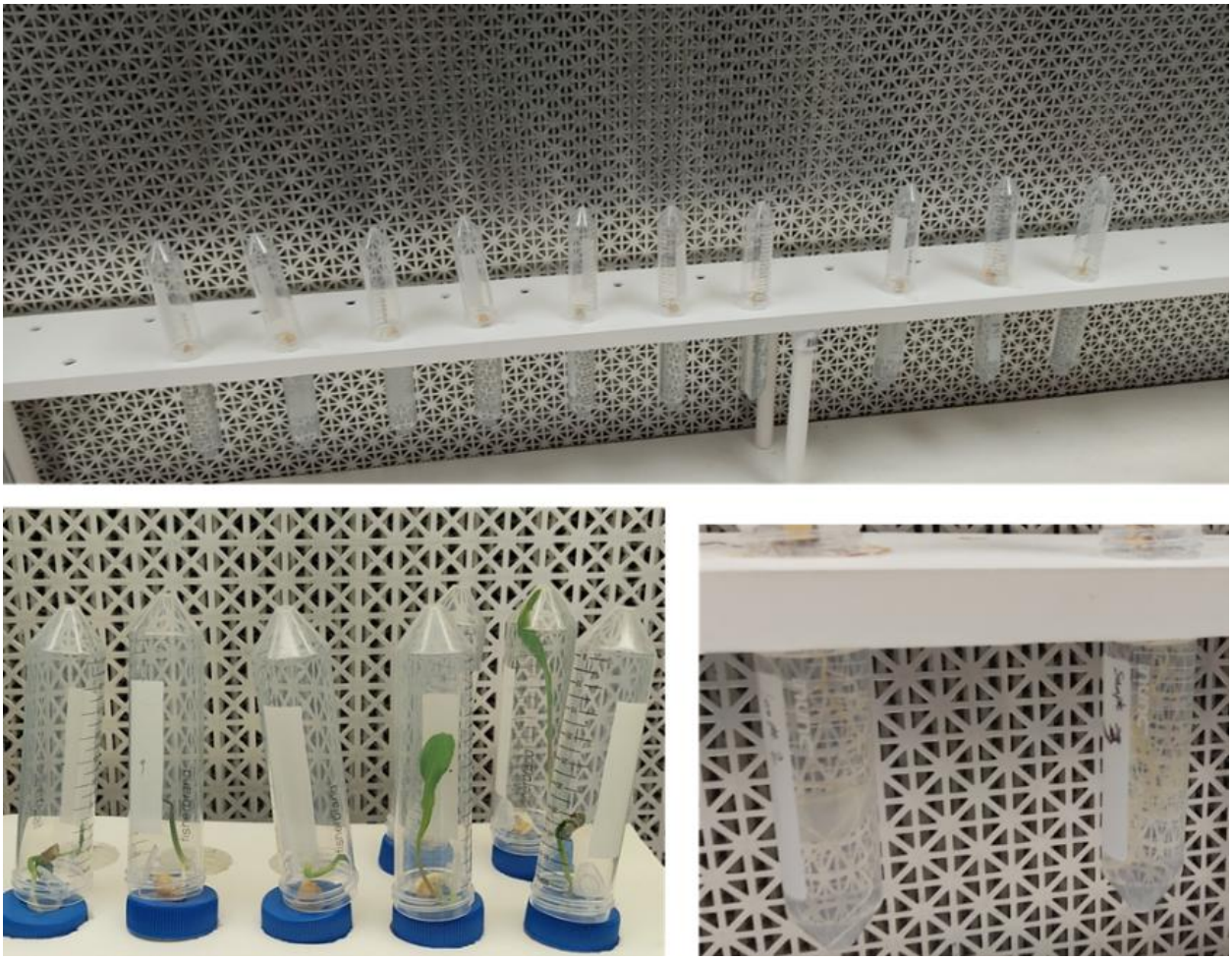

Figure 4.2. Scaffold System Setup for Maize Cultivation. The original setup for maize cultivation using individual propogating tubes (sterile 50-mL tubes) within a scaffold system, designed to support and organize plant growth while maintaining controlled environmental conditions and sterility.

After 14 days, the plants were ready for sampling. The roots were rinsed with DI water twice before being soaked in 50 mL of fresh *N. europaea* media for 24 h. Plants were rinsed after incubation and placed in their original nutrient solution.

Experiment 1b. Screening Cultivars

N. europaea cells were grown in batch and harvested as described above in Chapter 2, General Setup. The cells were resuspended in 10 mL of root exudate medium to obtain an OD_{600}

of 0.09 within the 50-mL Erlenmeyer flask. Samples were conducted in triplicate. Flasks were wrapped in foil and incubated for 1 hour at 30°C in the dark with continuous shaking at 120 rpm. NO_2^- measurements were taken at 0, 1, 2, 4, and 6 hours after incubation.

Experiment 2: Optimized Protocol for BNI Screening

Experiment 2a. Hydroponic Cultivation of Maize Cultivars

The germination procedure for the optimized protocol is identical to that described in Experiment 2a above. However, the hydroponic setup was upgraded to better accommodate larger root biomass and provide more consistent cultivation (Figure 4.3). Following germination, the seedlings were transferred to a greenhouse-based hydroponic system equipped with aeration. This system utilized high-impact polypropylene tanks with a capacity of 120 L. Each tank was covered with a Styrofoam lid containing 35 evenly spaced holes. Within each hole, a PVC pipe with perforations allowed aeration—provided by four air pumps—to reach the root zone and serve as a scaffold for each plant. Germinated seedlings, initially grown in plugs, were transferred into heavy-duty black net pots for structural support.

Each tank was filled with 100 L of modified nutrient solution composed of: 281 μM KH_2PO_4, 178 μM K_2SO_4, 71 μM $CaCl_2 \cdot 2H_2O$, 150 μM $MgSO_4 \cdot 7H_2O$, 41 μM Fe-EDTA, 922 μM H_3BO_3, 0.3 μM $CuSO_4 \cdot 5H_2O$, 9.1 μM $MnSO_4 \cdot 6H_2O$, 5.2 μM $Na_2MoO_4 \cdot 2H_2O$, and 7.7 μM $ZnSO_4 \cdot 7H_2O$. Plants were provided with ammonium nitrate (NH_4NO_3) as a N source. The nutrient solution was replaced with fresh solution every 7 days and the pH was adjusted daily to be in the range of 6.0 and 6.5 with 1 N HCl or 1 N NaOH. Between plantings, the system was sanitized with 30% hydrogen peroxide to minimize contamination and ensure consistent growing conditions.

Figure 4.3. Hydroponic System Setup and Root Biomass. The upgraded hydroponic system designed to support larger root biomass and provide more consistent conditions for maize cultivation.

Root exudates were collected nondestructively at various time points, ranging from 14 days to 2 months post-germination. Prior to collection, the roots were rinsed with DI water for 2-3 minutes. The exudates were collected by placing 100 mL of fresh *N. europaea* media in a sterile collection container beneath the roots for 24 h with aeration. After collection, plants were returned to the nutrient solution in the hydroponic tanks. Experiments were conducted on the same day of exudate collection, and any excess root exudate was stored in –80°C for future analysis, if necessary.

Experiment 2b. Screening Cultivars

N. europaea cells were grown in batch and harvested as described above in Chapter 2, General Setup. Upon final centrifugation, the cells were resuspended in the root exudate medium to obtain an OD_{600} of 0.1 for *N. europaea* within the well. In a 96-well plate, 300 µL of the *N. europaea* and root exudate mixture was added to each well in triplicate. Wells containing *N. europaea* with fresh medium served as the positive control. Wells with only the root exudate served as the negative control and were monitored to ensure background NO_2^- remained low over time. Two microplates were prepared: one for the initial NO_2^- measurement (0 h) and one for the final measurement (1 h). Samples were incubated for 1 hour at 30°C in the dark with continuous shaking at 120 rpm. At each time point, 20 µL of 0.1 M AT was added as a stop solution to prevent additional NO_2^- from forming in the 30-minute incubation period for the Griess reagent. Samples that contained initial NO_2^- concentrations exceeding 200 µM were excluded from analysis to minimize interference from background NO_2^- in the root exudate samples. Additionally, samples were excluded if the negative control increased more than 100 µM within the hour, as such a substantial increase in NO_2^- concentrations could indicate potential contamination or experimental error, which could distort the analysis of experimental samples. An increase greater than 100 µM is considered abnormal based on previous experiments and data from negative controls. The inhibitory effect was determined to be a ratio between the experimental net NO_2^- and the control net NO_2^-, as seen in Equation 4.1. For each set of experimental samples, the inhibitory effect was expressed as a % of the positive control, where the control is treated as 0% inhibition.

Eq 4.1. $$Percent\ Inhibition = \left(1 - \frac{Average\ Net\ Nitrite\ of\ Maize\ Sample}{Average\ Net\ Nitrite\ of\ Positive\ Control}\right) * 100$$

Experiment 2c. Conversion to AT Units

For ease of comparison across treatments, maize BNI activity was converted into AT units (ATU). Using the inhibition curve for AT in Chapter 2, 0.56 µM of AT an OD_{600} 0.1 resulted in 80% nitrification inhibition, and is defined as being 1 AT unit (ATU) of BNI activity (Equation 4.2). Using this reference point, the inhibitory effects observed in maize root exudates were quantified and expressed in ATUs to standardize BNI activity across cultivars and facilitate direct comparisons between cultivars and known inhibitors.

Eq. 4.2. $$ATU = \frac{Cultivar\ Inhibition}{80}$$

*1 ATU = 0.56 µM AT responsible for 80% inhibition

Experiment 2d. Statistical Analysis

Statistical analysis was conducted using three biological replicates per maize cultivar sample. To assess the influence of maize growth stage on BNI activity, a two-way analysis of variance (2-way ANOVA) was utilized in GraphPad Prism 10 (Boston, MA). A p-value of <0.05 was considered statistically significant for all analyses. Data were presented as means ± standard deviation (SD) for clarity.

Results and Discussion

BNI Screening Protocol Optimization

Optimizing the protocol for screening BNI activity was an iterative process. This section outlines the effects of various experimental modifications on BNI screening efficiency and accuracy, highlighting key adjustments that improved both protocol reliability and throughput.

Effect of Scaling Down to 96-Well Microplates (Iteration 1)

Initial screening experiments in 50-mL Erlenmeyer flasks were resource- and time-intensive. Each sampling required a large number of flasks, and NO_2^- measurements were laborious and time-consuming. Additionally, the small root mass of maize cultivars made it

difficult to collect sufficient root exudates for analysis. To address these challenges, the experiment was transitioned to a 96-well microplate format. Each well contained 300 µL of *N. europaea* (OD_{600} = 0.09) and root exudate medium, with samples conducted in triplicates. This transition significantly improved efficiency, reducing resource consumption and allowing for higher throughput screening. The microplate format reduced the required volume of root exudate to 2-3 mL per sample, facilitating higher throughput while maintaining assay sensitivity. Several maize cultivars could be tested simultaneously under identical conditions, streamlining the workflow and enabling faster data collection.

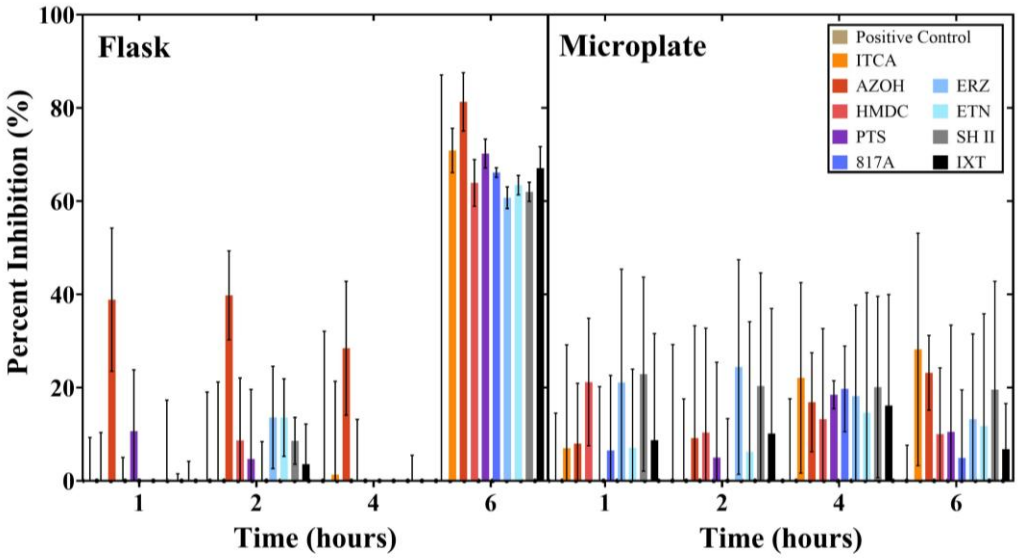

Figure 4.4. Comparison between 50-mL flask and 96-well microplate BNI screening methods. Inhibition percentages of positive control and 9 maize cultivars over 6 hours (n = 3). Error bars indicate the standard deviation of inhibition.

Both methods demonstrated that ITCA, AZOH, and PTS maize cultivars have the highest BNI potential. The flask method resulted in higher inhibition at the 6-hour time point, potentially due to greater initial bacterial activity and a larger reaction volume (Figure 4.4). In contrast, the

microplate maintained inhibition values around 25% over time, suggesting a more stable inhibition pattern.

While the microplate method demonstrated slightly higher variability, it was preferred due to its ease of handling, more consistent inhibition over time, and the practicality of limited root exudate collection. Further investigation revealed that inconsistent mixing before NO_2^- quantification was a source of error and that proper mixing was critical to improve accuracy. Unlike the flask method, where larger volumes naturally facilitated more uniform distribution, especially while on the shaker, the microplate wells had limited liquid volume, increasing the likelihood of concentration differences throughout the well. Proper mixing prior to measurement was identified as a critical factor for improving precision. Subsequent iterations incorporated mixing techniques, including gentle pipetting and brief plate shaking, to ensure homogeneity before NO_2^- quantification. Overall, due to its efficiency, reproducibility, and compatibility with limited root exudate volumes, the 96-well microplate method was the preferred BNI screening method.

Effect of Washing Cells Prior to Screening (Iteration 2)

To reduce background variability of NO_2^- measurements and improve the reliability of BNI screening, a washing step was added to remove residual NO_2^- from bacterial cultures. Prior to this modification, accumulated NO_2^- from previous bacterial activity contributed to background interference, complicating the accurate detection of inhibition effects. The presence of pre-existing NO_2^- in the media could lead to overestimated NO_2^- concentrations, reducing the sensitivity of the assay in detecting subtle changes due to BNI compounds. By implementing a standardized wash step, initial NO_2^- concentration decreased by 90%, from an average of 315 µM to 30 µM present within the positive control (Figure 4.5). The dramatic decrease in baseline

NO_2^- levels ensured that measured NO_2^- accumulation during the assay was primarily due to real-time bacterial activity rather than carryover from prior growth. This adjustment improved both precision and reproducibility across experimental replicates. By minimizing background interference, the assay became more sensitive to detecting inhibition effects, leading to more reliable BNI activity assessments. The addition of the wash step was a crucial improvement in refining the screening process.

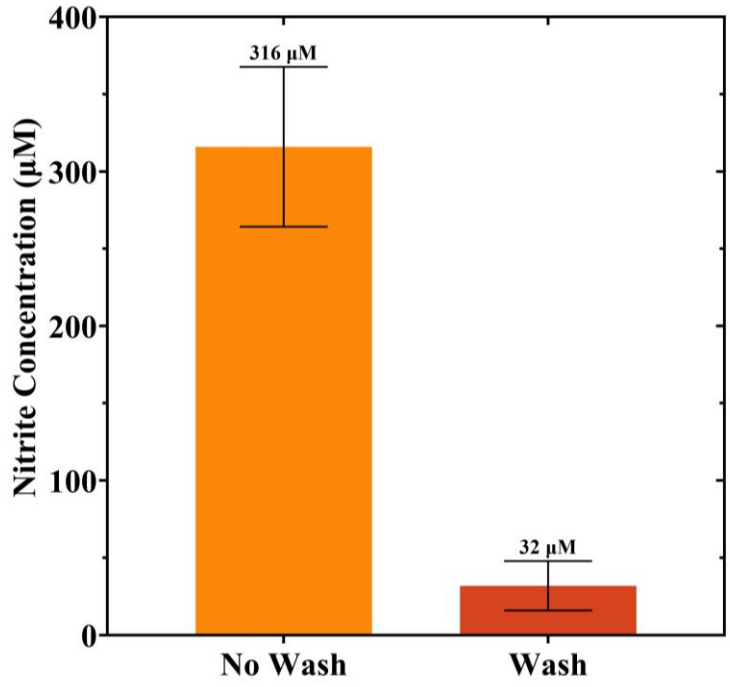

Figure 4.5. Impact of wash step on initial NO_2^- concentration. Initial NO_2^- concentrations in positive control of maize experiments with and without a wash step (n = 3). Error bars indicate the standard deviation while numerical values above error bars indicate the mean NO_2^- concentration (µM).

Effect of Stop Solution Addition (Iteration 3)

With the background NO_2^- levels significantly decreased, another improvement was made to enhance the accuracy of NO_2^- measurement. The incorporation of a stop solution (20 µL

of 0.1 M Allylthiourea) effectively prevented continued NO_2^- accumulation during the 30-minute Griess assay incubation. Other studies also utilized AT as a stop solution to prevent excess NO_2^- accumulation (O'Sullivan et al., 2016; Subbarao, Ishikawa, et al., 2006). By adding a sufficient concentration of AT, nitrification could be halted completely before measurement.

Without this intervention, residual bacterial activity could have led to ongoing NO_2^- production after sample collection, skewing the results. By halting nitrification at a precise point, this adjustment minimized variability and ensured that the measured NO_2^- concentrations accurately reflected the inhibitory effects under investigation. Consequently, this modification enhanced overall precision and reliability of NO_2^- quantification, contributing to more accurate BNI screening results.

Effect of Increasing Target Optical Density (Iteration 4)

Increasing the target optical density (OD_{600}) from 0.015 to 0.1 was an important modification that improved the consistency of biomass collection. This change allowed for more reliable inhibition measurements by ensuring higher bacterial cell concentration. At a higher OD_{600}, *N. europaea* exhibited more pronounced biomass, making it easier to collect a consistent and visible amount for the assay. After centrifuging, the visual confirmation of biomass ensured enough bacterial cells were present in the assay for accurate NO_2^- production and inhibition measurement.

Initially, there were concerns regarding the biomass concentration to root exudate volume ratio. In the 50-mL flasks, this ratio was 0.009 OD_{600}/mL (0.09 OD_{600}/10 mL), whereas in the 96-well microplate it increased to 0.3 OD_{600}/mL (0.09 OD_{600}/300 µL). This shift represented a 33-fold increase in biomass-to-BNI volume ratio, indicating that biomass in the 96-well microplate heavily outweighed the BNI volume. To investigate the impact of biomass

concentration, lower OD_{600} values of 0.045 and 0.015 were tested. However, working with such a low biomass levels presented challenges, particularly in ensuring uniform cell distribution after centrifugation. It was difficult to recover visible biomass adhering to the centrifuge tubes (Figure 4.6), leading to potential inconsistencies in the final biomass concentrations. Such variability could impact NO_2^- production, as lower biomass levels are associated with reduced metabolic activity and, consequently, less NO_2^- production. This reduction in activity may result in lower nitrite accumulation, which could be misinterpreted as increased nitrification inhibition. Ultimately, the biomass concentration was increased to 0.1 OD_{600} for subsequent experiments. This adjustment improved the uniformity of resuspended cultures, reduced variability across replicates, and improved confidence in NO_2^- measurements. Overall, the higher biomass concentration enabled more reliable assessment of BNI activity by maintaining consistent bacterial populations across experiments.

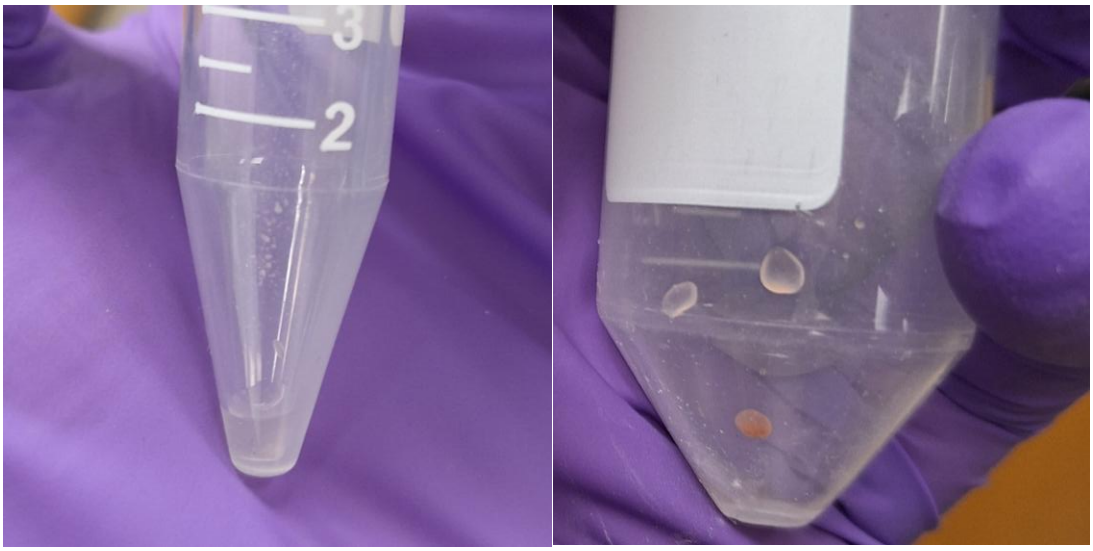

Figure 4.6. Visible biomass after centrifugation. Comparison of target OD_{600} values of 0.015 (left) and 0.1 (right), illustrating the increased biomass after centrifugation of 0.1 OD_{600}.

Effect of Maize Hydroponic System (Iteration 5)

Despite the previous modifications, variability in results persisted, largely due to significant differences in plant size, root biomass, and overall plant health. In response, the final iteration of the screening process involved transitioning maize cultivation from a small-scale scaffold setup to a larger hydroponic system. The initial method yielded insufficient root mass, leading to low BNI activity and high variability between plants. By switching to the hydroponic system, more consistent growth conditions were provided and root biomass significantly increased (Figure 4.7). This improvement enhanced the reliability of BNI screening.

Figure 4.7. Significant root biomass from updated hydroponic system. Root biomass development observed in samples at 28 days post-germination, with an emphasis on high growth observed across cultivars (Manitoba Yellow, Kiwase, and N6).

However, a large-scale hydroponic system requires careful monitoring and management to ensure conditions remained as consistent as possible. Unfortunately, during one round of

sampling, it was noted that some of the collected root exudate samples exhibited a green tint, indicating the presence of algae contamination (Figure 4.8). This posed a challenge as algae could interfere with the growth of *N. europaea* and the accuracy of inhibition measurements. To mitigate this issue, adjustments were made to the system to ensure proper maintenance. Despite this issue, the hydroponic system has proved to be an effective cultivation method for increasing root biomass and evaluating BNI activity.

Figure 4.8. Algal contamination from hydroponic system. Green-tinted samples suggest algal growth contamination in hydroponic system.

Final Optimized Protocol Performance

After adjusting the protocol through the above iterations, the final optimized protocol proved to be effective in generating more consistent inhibition trends across different maize cultivars. The refinement process addressed issues related to root biomass, sample handling, and NO_2^- accumulation. The updated methodology allowed for high-throughput screening without compromising the sensitivity or accuracy of the results. By streamlining the procedures and minimizing errors, the optimized protocol ensures that future screening experiments can be conducted with confidence.

Comparison to Existing Methods

This BNI screening method shares similarities to other techniques currently in use, as they all aim to enhance the efficiency and accuracy of assessing root exudates and their BNI

activity. However, this BNI screening method introduces several unique elements that set it apart from conventional methods.

One notable difference is its simplified sample preparation process. Unlike other methodologies, which involve vacuum evaporation and treatment with DMSO of root exudates to concentrate and isolate BNI compounds (Ishikawa et al., 2003; Otaka et al., 2023), this optimized method bypasses those resource-intensive steps. Instead, it directly adds root exudate samples to the bacteria, significantly reducing both the time and resources required for the screening process. This not only speeds up the overall process, but also makes it more scalable and cost-effective, particularly in high-throughput screenings.

Additionally, this BNI screening method produces more holistic results, as the root exudate sample may contain other compounds that aid in nitrification or inhibition. The interactions in the rhizosphere are very complex and difficult to isolate, making this broad approach beneficial. One limitation of this method, though, is that it does not ensure that hydrophobic BNI compounds are extracted from the root sample. Thus, a further improvement to this method could include a way to collect hydrophobic compounds, potentially through soaking in another solution and combing them all.

BNI Capacity in Maize Cultivars Across Growth Stages

Using the optimized protocol, the bioassay confirmed that the tested maize cultivars, KSU17 and B104, exhibited measurable BNI activity. While the inhibition levels were measurable, they were not substantial, generally not exceeding 0.625 ATU (50% inhibition). However, root exudates collected at various growth stages (21, 28, 30, and 45 days post-germination) revealed that BNI activity may be influenced by plant development.

At 21 days post-germination, KSU17 exhibited high BNI activity with an average of 0.558 ATU, corresponding to the V4-V6 stages of maize development when rapid nutrient uptake supports stalk growth (Ciampitti et al., 2016). However, BNI activity in KSU17 declined with plant age, dropping from 0.558 ATU at 21 days to 0.163 ATU at 45 days (Figure 4.9). This suggests that BNI activity may be developmentally regulated, potentially linked to changes in root biomass, structure, metabolic activity, or nutrient demand over time. In contrast, B104 showed a more moderate and consistent BNI profile over time, with inhibition levels ranging from 0.397 ATU at 28 days to 0.268 ATU at 45 days. Notably, B104 was not sampled at 21 days, so a direct comparison with KSU17 at this early stage could not be made. Additional sampling at earlier growth stages would help clarify if B104 follows a similar developmental pattern with higher BNI activity at early stages or if it exhibits a distinct inhibition pattern.

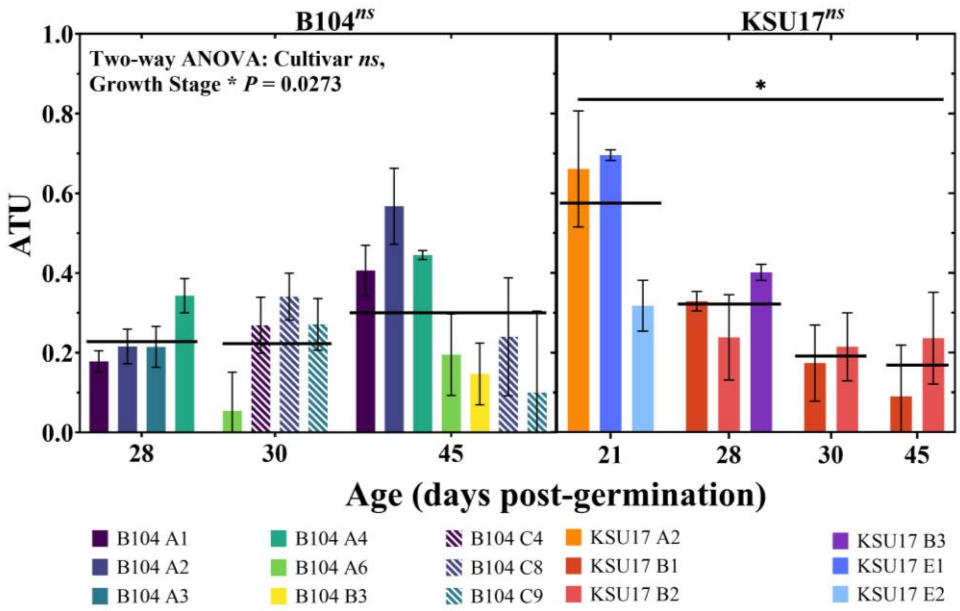

Figure 4.9. ATU of maize cultivars at various growth stages. Inhibition was converted to ATU, with 1.0 ATU equaling 80% inhibition from 0.56 µM AT. The black line for each set of samples represents the mean ATU value for those samples. Data were collected from biological replicates (n = 3), and error bars represent the standard deviation.

A two-way ANOVA between B104 and KSU17 at 28, 30, and 45 days revealed that growth stage had a significant effect on BNI activity ($F = 3.91$, $p = 0.0413$), while cultivar type did not ($F = 1.80$, $p = 0.1989$). More detailed results and supporting data can be found in Appendix D. Although numerical differences in inhibition were observed between cultivars, they were not statically significant at the selected time points. This is likely due to the high variability among samples, which may stem from differences in root biomass, overall plant health, or root characteristics. It is worth mentioning that root exudate samples varied in color, and root biomass differed between plants. Additional data on the maize cultivars, along with a more in-depth analysis, is needed to better understand the impact of these physical differences.

Limitations and Sources of Error

One of the main limitations of this study was time. Preparing the maize samples and growing the plants to a suitable stage for sampling typically requires several weeks to months, which significantly impacted the overall timeline of this study. Germinating seeds presented an additional challenge, as not all seeds sprouted uniformly, occasionally requiring repeat germination efforts and delaying downstream steps. Additionally, due to the iterative nature of protocol optimization process, it took serval months to determine the most effective approach. This process involved fine-tuning several variables and testing different conditions to ensure accuracy. To properly assess whether adjustments improved the screening process, the same cultivars had to be tested repeatedly. This added to the timeline, as testing of the same cultivar often took several weeks due to the need for consistent germination and collection of root exudates at specific growth stages. While this protocol has now been established, it is expected to continue evolving as more maize cultivars are screened and further improvements are made. Nevertheless, establishing a reliable screening protocol represents a significant milestone in

advancing this project, as it helps streamline the screening process and enables high-throughput analysis. By improving efficiency, this optimized approach opens up possibilities for more comprehensive and rapid evaluations of various cultivars.

Future Research

Future research will focus on expanding the scope of screenings to include additional maize cultivars, with the goal of identifying those that exhibit the highest BNI activity. A critical area of investigation will be determining the optimal time for sample collection to ensure the most accurate representation of root exudates and their associated biological activities. Preliminary studies have indicated a difference in BNI activity based on the growth stage. Additionally, once cultivars with the highest BNI activity are identified, they will undergo further research, including detailed genomic studies. This will involve isolating and characterizing the specific genes responsible for the BNI activity, providing deeper insights into the genetic basis of this trait. Understanding these genetic factors will enable targeted breeding programs to develop an elite maize cultivar with enhanced BNI activity.

Conclusions

The optimized BNI screening method developed in this study offers a promising approach for evaluating maize cultivars and their BNI activity, with notable advantages in efficiency, scalability, and cost-effectiveness. Preliminary findings indicate that both B104 and KSU17 exhibited BNI, with values ranging from 0.558 to 0.163 ATU. While numerically different, B104 and KSU17 are not statically different in their BNI activity. Analysis also suggested that growth stage has a significant impact on BNI activity, with younger plants producing more inhibition. Further investigation is needed to confirm this relationship and explore the underlying mechanisms. By refining the BNI screening protocol, this study lays the

groundwork for higher throughput screening and effective the way for more effective strategies in sustainable N management. Additionally, this quick and efficient screening method can be adapted for use with other plant species to identify and compare their BNI potential, broadening its applicability in future research and agricultural practices.

Chapter 5 - Overall Discussion and Conclusion

Effective and sustainable N management remains a critical challenge in agriculture, and BNI offers a promising strategy to address it. This study emphasizes the complexity of nitrification inhibition by different BNI compound and highlights the importance of biomass concentration in shaping inhibition responses. Compounds such as AT and MHPP consistently demonstrated strong inhibitory effects across biomass levels, while 1,9-D and LA required much higher concentrations to achieve similar levels of inhibition. Notably, 1,9-D exhibited the most pronounced biomass-dependent effect, with IC_{50} values increasing more than 5-fold between low and high OD_{600} values. These findings suggest that inhibition mechanisms are closely linked with microbial density, metabolic buffering, and compound structure. The inhibition data for AT was similar to previous studies; however, 1,9-D and MHPP displayed vast differences across studies with bioluminescent strains and OD_{600} values. Additionally, the reversibility of inhibition was also examined. While all compounds demonstrated some degree of recovery, 1,9-D showed complete reversibility, with nitrification activity fully restored within 2 hours of removal. AT, MHPP, and LA also showed reversibility, though cultures experiences temporary reductions in nitrification following removal, indicating residual metabolic disruption rather than permanent damage.

Furthermore, this study revealed that exposure to BNI compounds triggers a genetic response in *N. europaea*, primarily through changes in *amoA* gene expression. Significant decreases in *amoA* expression were observed in 1,9-D and MHPP, corresponding to nitrification rates of 63% and 76%, respectively. These reductions in gene expression indicate that BNI exposure disrupts the traditional pathway for *amoA*. Ongoing RNA sequencing efforts and

analysis will provide further insight into these regulatory mechanisms and impact on *N. europaea*.

While these studies quantified inhibition and provided insight into the mechanisms of BNI, it is important to apply this knowledge to the real-world and in the agriculture sector. Thus, another aspect of this study was screening maize cultivars for BNI activity. To do so effectively, an optimized protocol was created through an iterative process. The optimized protocol is efficient, scalable, and cost-effective for evaluating maize cultivars. Modifications to the protocol consisted of transitioning from 50-mL flasks to a 96-well microplate, addition of a wash step, addition of a stop solution, adjusting the target optical density, and upgrading to a larger hydroponic system. The developed screening approach offers valuable insights for advancing sustainable N management by enabling rapid identification of BNI capacity crop varieties and could be extended into other plant species. Preliminary results have identified B104 and KSU17 as having BNI potential, with levels ranging from 0.558 to 0.163 ATU. Interestingly, BNI activity appeared to be associated with plant growth stage, with younger plants exhibiting higher inhibition; however, further investigation is needed to confirm this trend. This optimized maize screen protocol will help identify additional cultivars for further investigation into the genes associated with BNI.

With the continued research and development of BNIs, the impact on N management in agriculture could be substantial. By identifying plant varieties with high BNI potential, it will be possible to develop crops that can naturally suppress nitrification and improve NUE. The knowledge gained from these studies, combined insights from the screening protocol and transcriptomic analysis of *N. europaea*, will inform future agricultural practices. By obtaining a better understanding of the mechanisms and interactions present within the soil, targeted

solutions can be created to improve sustainability in agriculture. In conclusion, this study has laid a solid foundation for the continued research and development of BNIs as a promising solution in agricultural N management. The integration of BNI research with genetic, ecological, and agronomic approaches has the potential to transform sustainable agricultural practices, reducing GHG emissions and improving NUE while enhancing food security.

References

Actor, J. K. (2012). Basic Bacteriology. *Elsevier's Integrated Review Immunology and Microbiology*, 93–103. https://doi.org/10.1016/B978-0-323-07447-6.00011-9

Arp, D. J., Sayavedra-Soto, L. A., & Hommes, N. G. (2002). Molecular biology and biochemistry of ammonia oxidation by Nitrosomonas europaea. *Archives of Microbiology*, *178*(4), 250–255. https://doi.org/10.1007/S00203-002-0452-0/METRICS

Bazhenov, S. V., Novoyatlova, U. S., Scheglova, E. S., Prazdnova, E. V., Mazanko, M. S., Kessenikh, A. G., Kononchuk, O. V., Gnuchikh, E. Y., Liu, Y., Al Ebrahim, R., Zavilgelsky, G. B., Chistyakov, V. A., & Manukhov, I. V. (2023). Bacterial lux-biosensors: Constructing, applications, and prospects. *Biosensors and Bioelectronics: X*, *13*, 100323. https://doi.org/10.1016/J.BIOSX.2023.100323

Bennett, K., Sadler, N. C., Wright, A. T., Yeager, C., & Hyman, M. R. (2016). Activity-Based Protein Profiling of Ammonia Monooxygenase in Nitrosomonas europaea. *Applied and Environmental Microbiology*, *82*(8), 2270. https://doi.org/10.1128/AEM.03556-15

Boline, A. (2024, March 27). *Fertilizer share of expected corn production expenses drops back after 2021–22 spike | Economic Research Service*. https://www.ers.usda.gov/data-products/charts-of-note/chart-detail?chartId=108828

Chen, G., Srinivasa Ranga, V. P., Mao, Y., Chen, K., & Qiao, H. (2008). Impact of lux gene insertion on bacterial surface properties and transport. *Research in Microbiology*, *159*(2), 145–151. https://doi.org/10.1016/J.RESMIC.2007.11.012

Ciampitti, I. A., Elmore, R. W., & Lauer, J. (2016, June). *Corn Growth and Development*. https://bookstore.ksre.ksu.edu/item/corn-growth-and-development-poster-20x30_MF3305

Clark, D. P., Pazdernik, N. J., & McGehee, M. R. (2019). Regulation of Transcription in Prokaryotes. *Molecular Biology*, 522–559. https://doi.org/10.1016/B978-0-12-813288-3.00016-1

Degrand, L., Garcia, R., Crouvisier Urion, K., & Guiga, W. (2023). Dynamic light scattering for the determination of linoleic acid critical micelle concentration. Effect of pH, ionic strength, and ethanol. *Journal of Molecular Liquids*, *388*, 122670. https://doi.org/10.1016/J.MOLLIQ.2023.122670

Erisman, J. W., Galloway, J. N., Seitzinger, S., Bleeker, A., Dise, N. B., Roxana Petrescu, A. M., Leach, A. M., & de Vries, W. (2013). Consequences of human modification of the global nitrogen cycle. *Philosophical Transactions of the Royal Society B: Biological Sciences*, *368*(1621). https://doi.org/10.1098/RSTB.2013.0116

Fowler, D., Coyle, M., Skiba, U., Sutton, M. A., Cape, J. N., Reis, S., Sheppard, L. J., Jenkins, A., Grizzetti, B., Galloway, J. N., Vitousek, P., Leach, A., Bouwman, A. F., Butterbach-Bahl, K., Dentener, F., Stevenson, D., Amann, M., & Voss, M. (2013). The global nitrogen cycle in the Twentyfirst century. *Philosophical Transactions of the Royal Society B: Biological Sciences*, *368*(1621). https://doi.org/10.1098/RSTB.2013.0164

Goodkind, A. L., Thakrar, S. K., Polasky, S., Hill, J. D., & Tilman, D. (2023). Managing nitrogen in maize production for societal gain. *PNAS Nexus*, *2*(10). https://doi.org/10.1093/PNASNEXUS/PGAD319

Ishikawa, T., Subbarao, G. V., Ito, O., & Okada, K. (2003). Suppression of nitrification and nitrous oxide emission by the tropical grass Brachiaria humidicola. *Roots: The Dynamic Interface between Plants and the Earth*, 413–419. https://doi.org/10.1007/978-94-017-2923-9_40

Kaur-Bhambra, J., Wardak, D. L. R., Prosser, J. I., & Gubry-Rangin, C. (2022). Revisiting plant biological nitrification inhibition efficiency using multiple archaeal and bacterial ammonia-oxidising cultures. *Biology and Fertility of Soils*, *58*(3), 241–249. https://doi.org/10.1007/S00374-020-01533-1/FIGURES/3

Kim, H. S., Ham, S. Y., Jang, Y., Sun, P. F., Park, J. H., Hoon Lee, J., & Park, H. D. (2019). Linoleic acid, a plant fatty acid, controls membrane biofouling via inhibition of biofilm formation. *Fuel*, *253*, 754–761. https://doi.org/10.1016/J.FUEL.2019.05.064

Kowalchuk, G. A., & Stephen, J. R. (2001). Ammonia-oxidizing bacteria: A model for molecular microbial ecology. *Annual Review of Microbiology*, *55*(Volume 55, 2001), 485–529. https://doi.org/10.1146/ANNUREV.MICRO.55.1.485/1

Kumar, R., Parmar, B. S., Walia, S., & Saha, S. (2015). Nitrification Inhibitors: Classes and Its Use in Nitrification Management. *Nutrient Use Efficiency: From Basics to Advance*, 103–122. https://doi.org/10.1007/978-81-322-2169-2_8/TABLES/1

Li, T., Wang, Z., Wang, C., Huang, J., Feng, Y., Shen, W., Zhou, M., & Yang, L. (2022). Ammonia volatilization mitigation in crop farming: A review of fertilizer amendment technologies and mechanisms. In *Chemosphere* (Vol. 303). Elsevier Ltd. https://doi.org/10.1016/j.chemosphere.2022.134944

Lv, H., Ren, D., Yan, W., Wang, Y., Liu, H., & Shen, M. (2020). Linoleic acid inhibits Lactobacillus activity by destroying cell membrane and affecting normal metabolism. *Journal of the Science of Food and Agriculture*, *100*(5), 2057–2064. https://doi.org/10.1002/JSFA.10228

Maize – CIMMYT. (2025). https://www.cimmyt.org/work/maize-research/

Motulsky, H. J. (2025). *GraphPad Prism 10 Curve Fitting Guide - Nonlinear regression with Prism*. https://www.graphpad.com/guides/prism/latest/curve-fitting/reg_nonlinchoices.htm

Nardi, P., Laanbroek, H. J., Nicol, G. W., Renella, G., Cardinale, M., Pietramellara, G., Weckwerth, W., Trinchera, A., Ghatak, A., & Nannipieri, P. (2020). Biological nitrification inhibition in the rhizosphere: determining interactions and impact on microbially mediated processes and potential applications. *FEMS Microbiology Reviews*, *44*(6), 874–908. https://doi.org/10.1093/FEMSRE/FUAA037

Nitrous Oxide Emissions | US EPA. (2025, March 20). https://www.epa.gov/ghgemissions/nitrous-oxide-emissions

O'Sullivan, C. A., Duncan, E. G., Whisson, K., Treble, K., Ward, P. R., & Roper, M. M. (2017). A colourimetric microplate assay for simple, high throughput assessment of synthetic and biological nitrification inhibitors. *Plant and Soil*, *413*(1–2), 275–287. https://doi.org/10.1007/S11104-016-3100-1/FIGURES/6

O'Sullivan, C. A., Fillery, I. R. P., Roper, M. M., & Richards, R. A. (2016). Identification of several wheat landraces with biological nitrification inhibition capacity. *Plant and Soil*, *404*(1–2), 61–74. https://doi.org/10.1007/s11104-016-2822-4

Otaka, J., Subbarao, G. V., MingLi, J., Ono, H., & Yoshihashi, T. (2023). Isolation and characterization of the hydrophilic BNI compound, 6-methoxy-2(3H)-benzoxazolone (MBOA), from maize roots. *Plant and Soil*, *489*(1–2), 341–359. https://doi.org/10.1007/S11104-023-06021-7/FIGURES/10

Otaka, J., Subbarao, G. V., Ono, H., & Yoshihashi, T. (2022). Biological nitrification inhibition in maize—isolation and identification of hydrophobic inhibitors from root exudates.

Biology and Fertility of Soils, *58*(3), 251–264. https://doi.org/10.1007/S00374-021-01577-X/FIGURES/10

Pariasca Tanaka, J., Nardi, P., & Wissuwa, M. (2010). Nitrification inhibition activity, a novel trait in root exudates of rice. *AoB PLANTS*, *2010*, 14. https://doi.org/10.1093/AOBPLA/PLQ014

Penuelas, J., Coello, F., & Sardans, J. (2023). A better use of fertilizers is needed for global food security and environmental sustainability. *Agriculture and Food Security*, *12*(1), 1–9. https://doi.org/10.1186/S40066-023-00409-5/METRICS

Petroli, C. D., Subbarao, G. V., Burgueño, J. A., Yoshihashi, T., Li, H., Franco Duran, J., & Pixley, K. V. (2023). Genetic variation among elite inbred lines suggests potential to breed for BNI-capacity in maize. *Scientific Reports 2023 13:1*, *13*(1), 1–12. https://doi.org/10.1038/s41598-023-39720-3

Population | United Nations. (2024). https://www.un.org/en/global-issues/population

Radniecki, T. S., Dolan, M. E., & Semprini, L. (2008). Physiological and transcriptional responses of Nitrosomonas europaea to toluene and benzene inhibition. *Environmental Science and Technology*, *42*(11), 4093–4098. https://doi.org/10.1021/ES702623S/SUPPL_FILE/ES702623S-FILE003.PDF

Sands, R. (2024, November 5). *Agriculture accounted for an estimated 10.5 percent of U.S. greenhouse gas emissions in 2022 | Economic Research Service*. https://www.ers.usda.gov/data-products/charts-of-note/chart-detail?chartId=110340

Sedlacek, C. J., Giguere, A. T., Dobie, M. D., Mellbye, B. L., Ferrell, R. V., Woebken, D., Sayavedra-Soto, L. A., Bottomley, P. J., Daims, H., Wagner, M., & Pjevac, P. (2020). Transcriptomic Response of Nitrosomonas europaea Transitioned from Ammonia- to

Oxygen-Limited Steady-State Growth. *MSystems*, *5*(1). https://doi.org/10.1128/msystems.00562-19

Stein, L. Y., Sayavedra-Soto, L. A., Hommes, N. G., & Arp, D. J. (2000). Differential regulation of amoA and amoB gene copies in Nitrosomonas europaea. *FEMS Microbiology Letters*, *192*(2), 163–168. https://doi.org/10.1111/J.1574-6968.2000.TB09376.X

Subbarao, G., Ito, O., Sahrawat, K., Berry, W., Nakahara, K., Ishikawa, T., Watanabe, T., Suenaga, K., Rondon, M., & Rao, I. (2006). Scope and Strategies for Regulation of Nitrification in Agricultural Systems—Challenges and Opportunities. *Critical Reviews in Plant Sciences*, *25*(4), 303–335. https://doi.org/10.1080/07352680600794232

Subbarao, G. V., Ishikawa, T., Ito, O., Nakahara, K., Wang, H. Y., & Berry, W. L. (2006). A bioluminescence assay to detect nitrification inhibitors released from plant roots: A case study with Brachiaria humidicola. *Plant and Soil*, *288*(1–2), 101–112. https://doi.org/10.1007/s11104-006-9094-3

Subbarao, G. V., Kishii, M., Bozal-Leorri, A., Ortiz-Monasterio, I., Gao, X., Ibba, M. I., Karwat, H., Gonzalez-Moro, M. B., Gonzalez-Murua, C., Yoshihashi, T., Tobita, S., Kommerell, V., Braun, H. J., & Iwanaga, M. (2021). Enlisting wild grass genes to combat nitrification in wheat farming: A nature-based solution. *Proceedings of the National Academy of Sciences of the United States of America*, *118*(35), e2106595118. https://doi.org/10.1073/PNAS.2106595118/SUPPL_FILE/PNAS.2106595118.SAPP.PDF

Subbarao, G. V., Nakahara, K., Hurtado, M. P., Ono, H., Moreta, D. E., Salcedo, A. F., Yoshihashi, A. T., Ishikawa, T., Ishitani, M., Ohnishi-Kameyama, M., Yoshida, M., Rondon, M., Rao, I. M., Lascano, C. E., Berry, W. L., & Ito, O. (2009). Evidence for biological nitrification inhibition in Brachiaria pastures. *Proceedings of the National*

Academy of Sciences of the United States of America, *106*(41), 17302–17307. https://doi.org/10.1073/PNAS.0903694106

Subbarao, G. V., Nakahara, K., Ishikawa, T., Ono, H., Yoshida, M., Yoshihashi, T., Zhu, Y., Zakir, H. A. K. M., Deshpande, S. P., Hash, C. T., & Sahrawat, K. L. (2013). Biological nitrification inhibition (BNI) activity in sorghum and its characterization. *Plant and Soil*, *366*(1–2), 243–259. https://doi.org/10.1007/S11104-012-1419-9/TABLES/3

Subbarao, G. V., Nakahara, K., Ishikawa, T., Yoshihashi, T., Ito, O., Ono, H., Ohnishi-Kameyama, M., Yoshida, M., Kawano, N., & Berry, W. L. (2008). Free fatty acids from the pasture grass Brachiaria humidicola and one of their methyl esters as inhibitors of nitrification. *Plant and Soil*, *313*(1–2), 89–99. https://doi.org/10.1007/s11104-008-9682-5

Subbarao, G. V., Rondon, M., Ito, O., Ishikawa, T., Rao, I. M., Nakahara, K., Lascano, C., & Berry, W. L. (2007). Biological nitrification inhibition (BNI) - Is it a widespread phenomenon? *Plant and Soil*, *294*(1–2), 5–18. https://doi.org/10.1007/s11104-006-9159-3

Sun, L., Lu, Y., Yu, F., Kronzucker, H. J., & Shi, W. (2016). Biological nitrification inhibition by rice root exudates and its relationship with nitrogen-use efficiency. *New Phytologist*, *212*(3), 646–656. https://doi.org/10.1111/NPH.14057

Tarre, S., & Green, M. (2004). High-rate nitrification at low pH in suspended- and attached-biomass reactors. *Applied and Environmental Microbiology*, *70*(11), 6481–6487. https://doi.org/10.1128/AEM.70.11.6481-6487.2004/ASSET/B40396CE-7625-41F5-8F0F-0656981A1992/ASSETS/GRAPHIC/ZAM0110449620004.JPEG

USDA. (2021). *About the Survey*. http://quickstats.nass.usda.

Wang, X., Bai, J., Xie, T., Wang, W., Zhang, G., Yin, S., & Wang, D. (2021). Effects of biological nitrification inhibitors on nitrogen use efficiency and greenhouse gas emissions

in agricultural soils: A review. *Ecotoxicology and Environmental Safety*, *220*, 112338. https://doi.org/10.1016/J.ECOENV.2021.112338

Woodward, E. E., Edwards, T. M., Givens, C. E., Kolpin, D. W., & Hladik, M. L. (2021). Widespread Use of the Nitrification Inhibitor Nitrapyrin: Assessing Benefits and Costs to Agriculture, Ecosystems, and Environmental Health. *Environmental Science and Technology*, *55*(3), 1345–1353. https://doi.org/10.1021/ACS.EST.0C05732/ASSET/IMAGES/MEDIUM/ES0C05732_M001.GIF

Yildirim, S. C., Nathanael, J. G., Frindte, K., Leal, O. dos A., Walker, R. M., Roessner, U., Knief, C., Nicolas, B., & Wille, U. (2024). 4-Methyl-1-(prop-2-yn-1-yl)-1H-1,2,3-triazole (MPT): A Novel, Highly Efficient Nitrification Inhibitor for Agricultural Applications. *ACS Agricultural Science and Technology*, *4*(2), 255–265. https://doi.org/10.1021/ACSAGSCITECH.3C00506/ASSET/IMAGES/LARGE/AS3C00506_0006.JPEG

Yu, R., & Chandran, K. (2010). *Strategies of Nitrosomonas europaea 19718 to counter low dissolved oxygen and high nitrite concentrations*. http://www.biomedcentral.com/1471-2180/10/70

Yu, X., Keitel, C., Zhang, Y., Wangeci, A. N., & Dijkstra, F. A. (2022). Global meta-analysis of nitrogen fertilizer use efficiency in rice, wheat and maize. *Agriculture, Ecosystems & Environment*, *338*, 108089. https://doi.org/10.1016/J.AGEE.2022.108089

Zakir, H. A. K. M., Subbarao, G. V., Pearse, S. J., Gopalakrishnan, S., Ito, O., Ishikawa, T., Kawano, N., Nakahara, K., Yoshihashi, T., Ono, H., & Yoshida, M. (2008). Detection, isolation and characterization of a root-exuded compound, methyl 3-(4-hydroxyphenyl)

propionate, responsible for biological nitrification inhibition by sorghum (Sorghum bicolor). *New Phytologist*, *180*(2), 442–451. https://doi.org/10.1111/J.1469-8137.2008.02576.X

Appendix A - *Nitrosomonas europaea* Growing Conditions

Growing *Nitrosomonas europaea:*

Factors to Consider and the Recipe for Making Medium

From the Laboratory of Daniel J. Arp Oregon State University, Corvallis OR 97331, USA

Nitrosomonas europaea is an autotrophic nitrifying bacterium that gains all of its energy for growth from the oxidation of ammonia to nitrite as follows:

Equation: $2H^+ + 2e^- + NH_3 + O_2 \rightarrow NH_2OH + H_2O \rightarrow NO_2^- + 5H+ + 4e^-$

Most nitrifying bacteria have a relatively long generation time (8-72 hours) and their isolation from the environment is a long-drawn out process that may take up to 6 months. However, from an ATCC culture, or once they are growing, they are relatively easy to grow and keep viable. The ATCC 19718 *N. europaea* stock culture has a generation time of approximately 8 hours. There are several factors worth considering in successfully growing a nitrifying bacterium such as *N. europaea*. Lack of growth is usually due to an error in one or a combination of the following factors:

- **pH of the growth medium**. Ammonia (NH_3), not ammonium (NH_4^+; pKa= 9.25) is the natural growth substrate of *N. europaea*. The availability of ammonia, which is supplied as ammonium salts, is dependent on the pH of the medium. During growth, the medium becomes acidified (see equation), which results in a progressive decrease in the amount of free NH_3 in solution. In the laboratory, *N. europaea* is grown at a pH between 7.8 and 8.0 using a relatively strong buffer to minimize the drop in pH. If *N. europaea* is not growing reasonably well, a possible cause might be low pH.

- **Water quality**. *N. europaea* is relatively sensitive to metals. While one can grow them well on tap deionized water, more consistent results are obtained when using double distilled water. For example, *N. europaea* is sensitive to copper and zinc, so if it is not growing well, metal contamination might be the cause of poor growth (e.g. from distillation equipment, containers, faucets, etc.).

- **Rubber**. Because *N. europaea* is strictly lithotrophic; any compound that inhibits ammonia oxidation will hamper growth. Sulfur-containing compounds are very effective growth inhibitors and are found in unexpected places such as red-rubber stoppers. Many volatile sulfur compounds are used in the vulcanization of rubber and these compounds tend to leach out. Sulfur compounds can inhibit ammonia oxidation at concentrations as low as a few ppm.

- **Heterotrophic microorganisms**. Nitrifying bacteria may be preyed on by heterotrophic microorganisms as they grow or may excrete compounds that heterotrophic microorganisms can use for growth. Contamination with heterotrophic microorganisms is the bane of nitrifying cultures; once they contaminate a culture of nitrifying bacteria, they are hard to

eliminate. You may want to maintain several storage cultures that can be kept viable in a refrigerator for up to 2 months. It is also possible to store the cultures in DMSO (7%) or in Glycerol (35%) at -80°C for long-term storage.

- **Viability.** Propagate the cultures every three to four days with actively growing cells. Because 4-day old cells are close to peak activity, they will grow quickly in the fresh culture flasks, minimizing the likelihood of heterotrophic contamination. A culture started with cells from long-term storage (i.e. at -80°C in 7% DMSO or in 35% Glycerol) can take up to a month to show first appreciable growth.

- **Light.** Ammonia oxidation is inhibited by intense light. Consider wrapping the flasks in foil or incubating them in a darkened room if you are still having problems growing *N. europaea*.

The Medium Recipe for *N. europaea*

Step 1
Put 900 mL of deionized water in a 2 L Erlenmeyer flask.
Add in sequence:
3.3 g $(NH_4)_2SO_4$ (25 mM);
0.41 g KH_2PO_4 (3.3 mM)
0.75 mL 1 M $MgSO_4$ stock solution
0.2 mL 1 M $CaCl_2$ stock solution
0.33 mL 30 mM $FeSO_4$ /50 mM EDTA stock solution
0.01 mL 50mM $CuSO_4$ stock solution

Sterilize it using an autoclave

Step 2

Put 400 mL of deionized water in a beaker. Add:
1.49 g KH_2PO_4 (22 mM)
16.81 g K_2HPO_4
Adjust pH to 8.0 with 10 N NaOH and bring it to a final volume of 500 mL with deionized water. Sterilize in an autoclave in 100 mL fractions in 250-500 mL Erlenmeyer flasks.

Step 3
Prepare 500 mL of 5% (w/v) Na_2CO_3 (anhydrous)
Sterilize it using an autoclave

How to Grow *N. europaea*

1. Add 100 mL aliquot of solution prepared in Step 2 to the flask prepared in Step 1.
2. Add 8 mL of the solution prepared in Step 3 to the flask prepared in Step 1.
3. Divide the 1 L of media between two 2 L flasks (500 mL in each).
4. Finally add 50 ml of 3-day old culture to the flask prepared in Step 1, and incubate it on a rotary shaker (100-150 RPM) at 30°C. The bacterium should reach approximately OD_{600nm} ~0.1 in three to four days.

Appendix B - Dissolved Oxygen Calculation

Dissolved Oxygen (DO) Calculation:

$$C_{DO} = k_H(P_{O2})\left(\frac{V_{headspace}}{V_{media}}\right)$$

Where,

$C_{DO} = dissolved\ oxygen\ concentration\ in\ media\ (\frac{mg}{L})$

$k_H = Henry's\ Law\ Constant\ for\ oxygen = 1.5 \times 10^{-3}\frac{mol}{L}\ \ (at\ 30°C)$

$P_{O2} = Partial\ Pressure\ of\ oxygen\ in\ headspace = 0.21\ atm$

$V_{headspace} = Volume\ of\ the\ headspace = 60\ uL$

$V_{media} = Volume\ of\ the\ media = 300\ uL$

Assuming:

- Air-saturation
- k_H for pure water at 30°C

Thus,

$$C_{DO} = k_H(P_{O2})\left(\frac{V_{headspace}}{V_{media}}\right) = 1.5 \times 10^{-3}\frac{mol}{L}(0.21\ atm)\left(\frac{60\ uL}{300\ uL}\right) = 6.3 \times 10^{-5}\frac{mol}{L}$$

$$Convert\ to\ \frac{mg}{L}: 6.3 \times 10^{-5}\frac{mol}{L}\left(32{,}000\frac{mg}{mol}\right) = 2.016\frac{mg}{L} = C_{DO}$$

Appendix C - Primer Information

Appendix Table C.1. Primer Information

Target Gene	Primer Set	Primer Sequence (5' – 3')	Method
16S rRNA [1]	8F	AGAGTTTGATCCTGGCTCAG	1m@95,(45s@94,45s@50,1.5m@72)x 26,15m@72
	1492R	TACCTTGTTACGACTT	
Bacterial – *amoA* [2]	amoA-1F	GGGGTTTCTACTGGTGGT	5m@94, (60s@94, 90s@60, 90s@72), 10m@72, x 40cycle/ 30s@94, 15s
	amoA-2R	CCCCTCKGSAAAGCCTTCTTC	3m@95 x40(45s@95, 60s@57, 60s@72)10m@72

Abbreviations for degenerate nucleotide positions are as follows: K = G or T. 16S

[1] RI Amann, et al., Combination of 16s rrna-targeted oligonucleotide probes with flow cytometry for analyzing mixed 12 microbial populations. *Appl. Environ. Microbiol*. 56, 1919–1925 (1990).

[2] JH Rotthauwe, KP Witzel, W Liesack, The ammonia monooxygenase structural gene amoa as a functional marker: 29 molecular fine-scale analysis of natural ammonia-oxidizing populations. *Appl. PEnviron. Microbiol*. 63, 4704–4712 (1997).

Appendix D - Maize Statistical Analysis

Analysis with 28, 30, and 45 days where data is available for both B104 and KSU17.

Data analyzed: Average Inhibition of B104 and KSU17 at Various Growth Stages (28, 30, 45 days)

Source of Variation	Degrees of Freedom	Sum of Squares	Mean square
Column Factor	1	136.1	136.1
Row Factor	2	593.1	296.6
Interaction	2	26.33	13.16
Residual (error)	16	1212	75.77
Total	21	1938	

You have CHOSEN to perform this analysis without an interaction. This choice indicates that you expect the Column Factor to have the same effect (if any) at all levels of the Row Factor and vice versa.

Does Column Factor affect the result?

Column Factor accounts for 7.021% of the total variance.
F = 1.80. DFn = 1, DFd = 16
The P value = 0.1989
If Column Factor has no effect overall, there is a 20% chance of randomly observing an effect this big (or bigger) in an experiment of this size. The effect is considered not significant.

Does Row Factor affect the result?

Row Factor accounts for 30.6% of the total variance.
F = 3.91. DFn = 2, DFd = 16
The P value = 0.0413
If Row Factor has no effect overall, there is a 4.1% chance of randomly observing an effect this big (or bigger) in an experiment of this size. The effect is considered significant.

Appendix Table D.2. KSU17 and B104 Summary for 28, 30, and 45 days.

	KSU17			B104		
Days Post-Germination	Mean	SD	N	Mean	SD	N
28	25.8	6.5	3	31.76	8.5	4
30	15.5	2.3	2	17.758	11.9	3
45	13.02	2	2	21.471	9.4	8

Analysis including KSU17's inhibition data at 21 days.

Data analyzed: Average Inhibition of B104 and KSU17 at Various Growth Stages

Source of Variation	Degrees of Freedom	Sum of Squares	Mean square
Cultivar	1	155.0	155.0
Growth Stage	3	1970	656.8
Residual (error)	20	1796	89.82
Total	24	3834	

You have CHOSEN to perform this analysis without an interaction. This choice indicates that you expect the Cultivar to have the same effect (if any) at all levels of the Growth Stage and vice versa.

Does Cultivar affect the result?

Cultivar accounts for 4.041% of the total variance.
F = 1.73. DFn = 1, DFd = 20
The P value = 0.2039
If Cultivar has no effect overall, there is a 20% chance of randomly observing an effect this big (or bigger) in an experiment of this size. The effect is considered not significant.

Does Growth Stage affect the result?

Growth Stage accounts for 51.38% of the total variance.
F = 7.31. DFn = 3, DFd = 20
The P value = 0.0017
If Growth Stage has no effect overall, there is a 0.17% chance of randomly observing an effect this big (or bigger) in an experiment of this size. The effect is considered very significant.

Appendix Table D.2. KSU17 and B104 Summary for 21, 28, 30, and 45 days.

	KSU17			B104		
Days Post-Germination	Mean	SD	N	Mean	SD	N
21	44.63	16.7	3			
28	25.8	6.5	3	31.76	8.5	4
30	15.5	2.3	2	17.758	11.9	3
45	13.02	2	2	21.471	9.4	8